Where the Blue Stragglers Roam: The Link Between Formation and Environment

Where the Blue Stragglers Roam: The Link Between Formation and Environment in Globular Clusters

By

Nathan W. C. Leigh, B.Sc.

A Thesis

Submitted to the School of Graduate Studies

in Partial Fulfilment of the Requirements

for the Degree

Master of Science

McMaster University

MASTER OF SCIENCE (2007) McMaster University

(Department of Physics and Astronomy) Hamilton, Ontario

TITLE: Where the Blue Stragglers Roam: The Link Between Formation and Environment in Globular Clusters

AUTHOR: Nathan Leigh, B.Sc.

SUPERVISOR: Alison Sills

NUMBER OF PAGES: xi, 115

Abstract

The conditions ideally suited for blue straggler star formation are for the most part unknown, though there is mounting evidence to suggest that the preferred blue straggler formation pathway, whether it be via the coalescence of a primordial binary system or through the collision of two single main-sequence stars, depends largely on the cluster environment. In this thesis we are trying to isolate the preferred blue straggler formation mechanism(s) operating in various globular cluster environments by comparing relative blue straggler frequencies to global cluster properties.

We define a series of selection rules to isolate the blue stragglers from main-sequence turn-off and extended horizontal branch stars in the colour-magnitude diagrams of 57 globular clusters taken from HST images of their central cores. The boundary conditions were defined using only the main-sequence turn-off as a point of reference, and are hence applied consistently from cluster to cluster. We chose to count only those stars found within one core radius of the cluster center in an effort to obtain a sample that is approximately representative of a uniform cluster environment where, ideally, a single blue straggler formation mechanism is predominantly operating. Relative frequencies of blue straggler stars are then found using the red giant branch for normalization and are subsequently analyzed. We confirm the anticorrelation between relative blue straggler frequency and total integrated cluster luminosity previously observed by Piotto et al. (2004), and find a new anticorrelation between relative blue straggler frequency and the central velocity dispersion, as well as a weak anticorrelation with the half-mass relaxation time. We find

no other statistically significant trends. Observational implications pertaining to blue straggler formation mechanisms are then discussed.

We present a very simple, semi-analytic model designed in an attempt to reproduce the observed trends in the core. Using estimates for the collisional timescales, we find that only a small percentage of the blue straglers produced are a direct result of collisions. The majority of the blue stragglers created in our model are thus products of mass-transfer in tight, low-mass binary systems. We were surprised to find a reasonably good agreement between the data and our predictions, given the simplicity of our model. Our results suggest that the binary fraction could be a crucial parameter in shaping blue straggler populations, and hence better and more abundant observations of binary systems and their numbers could prove an important step in gaining a better understanding of blue straggler formation mechanisms.

Acknowledgements

I would like to thank my supervisor Dr. Alison Sills for her continued guidance, support and patience. She has been an excellent teacher, a phenomenal supervisor and an inspiration time and again. I cannot thank her enough.

I would also like to thank Dr. Bill Harris and Dr. Alan Chen, my Master's committee members, for their more than helpful comments and suggestions along the way, in addition to their patience and support.

Finally, I would like to thank my parents for their continued guidance and support, both with this project and with other related matters. They have always been there for me and it has not gone unnoticed.

Table of Contents

[1] Much of this chapter has already been published as Leigh, N., Sills, A., & Knigge, C. Where the Blue Stragglers Roam: Searching for a Link Between Formation and Environment, ApJ, accepted, 2007.

List of Figures

List of Tables

Chapter 1

Introduction

1.1 A Brief Introduction to Stellar Populations

Blue stragglers are mysterious stellar objects that have fueled a great deal of controversy regarding cluster dynamics and stellar evolution (e.g. Sills & Bailyn, 1999). The existence of these stars poses a few important questions, namely what goes on inside a star over the course of its life, and more generally, what goes on inside a cluster of stars? Equally as important, how are observations affected as a result of these internal and external processes? In asking these questions, we hope to gain better insight into the potentially complex machinery operating to create the BSSs that we observe in stellar populations.

Once a cloud of gas and dust has completed its first episode of star formation, the question of what comes next and, perhaps more importantly, how might the evolution of individual stars therein be affected requires an anything but straight forward answer. It seems that for some stars, the evolution will depend as much on their own initial conditions as it will on their surroundings.

Clusters come in a variety of different shapes and sizes and it is possible that some amongst them play favorites and are preferentially home to particular phenomena (Binney & Merrifield, 1998). Despite this, there are a few key features that all clusters share. For instance, the first stars in a given cluster were formed at roughly the same time, and are made from the collapse of the same gas cloud. Consequently, they tend to start their lives with similar compositions and it is their mass that determines the rate of evolution (Carroll & Ostlie, 2006). The larger a star, the quicker it evolves. Since clusters are home to a wide variety of stars having often drastically different masses, they typically harbour stars representing most, if not all, of the various phases of stellar evolution.

In setting out to understand the specifics of intricate and complex subjects, it is often beneficial to take a step back and have a look at the bigger picture. The theory of stellar evolution is no exception, and in attempting to piece together a satisfactory explanation of what exactly it is stars do in the billions of years they survive, it is often useful to look at what a given stellar population is doing as a whole. As such, we can turn to a cluster's colour-magnitude diagram (CMD), a plot of brightness (in absolute magnitude) versus colour or temperature, wherein each point represents a star residing in the cluster (Carroll & Ostlie, 2006). The distribution of points in a given cluster's CMD is anything but random. In fact, an approximate shape or sequence is apparent and can be consistently observed from cluster to cluster. As stars age they evolve, causing parameters like the composition, mass, temperature, luminosity and size to all change (e.g. Binney & Merrifield, 1998). As a result, the observable properties of stars are altered over the course of their lengthy lives

and it is the presence of such a large number of stars at different evolutionary stages that gives CMDs their characteristic shape.

In the CMDs of relatively young clusters, most stars lie on the main-sequence (MS) during which time hydrogen is being fused into helium in the core. As a stellar population ages, the bluer more massive stars at the upper left end of the main-sequence evolve quicker than the redder, less massive ones to the lower right. The upper end of the MS, called the main-sequence turn-off (MSTO), then marks the end of the core hydrogen-burning phase, at which time the helium core begins to collapse and heat up while the hydrogen-burning zone moves outwards into a shell that surrounds the core. The MS-lifetimes of the most massive stars still populating this evolutionary stage can be used to gauge the cluster age (Carroll & Ostlie, 2006).

As the core collapses, heat is generated and increases the overall pressure causing the star's outer envelope to expand and cool. Helium burning starts in the core when the temperature nears 10^8 K, and the star brightens and reddens as it begins its ascent up the Red Giant Branch (RGB) (Carroll & Ostlie, 2006). Eventually, it will re-enter a phase of hydrostatic and thermal equilibrium and will move onto the horizontal branch (HB). Here, stars continue to undergo core helium fusion, thus stimulating the build-up of carbon and oxygen. Figure 1.1 shows the CMD for the old globular cluster NGC 362; each of the major stages of stellar evolution are represented.

While stellar evolution is indeed a crucial factor in understanding and interpreting CMDs, it seems as though there are other factors at work in shaping the characteristic trends that we see. Upon broadening our view

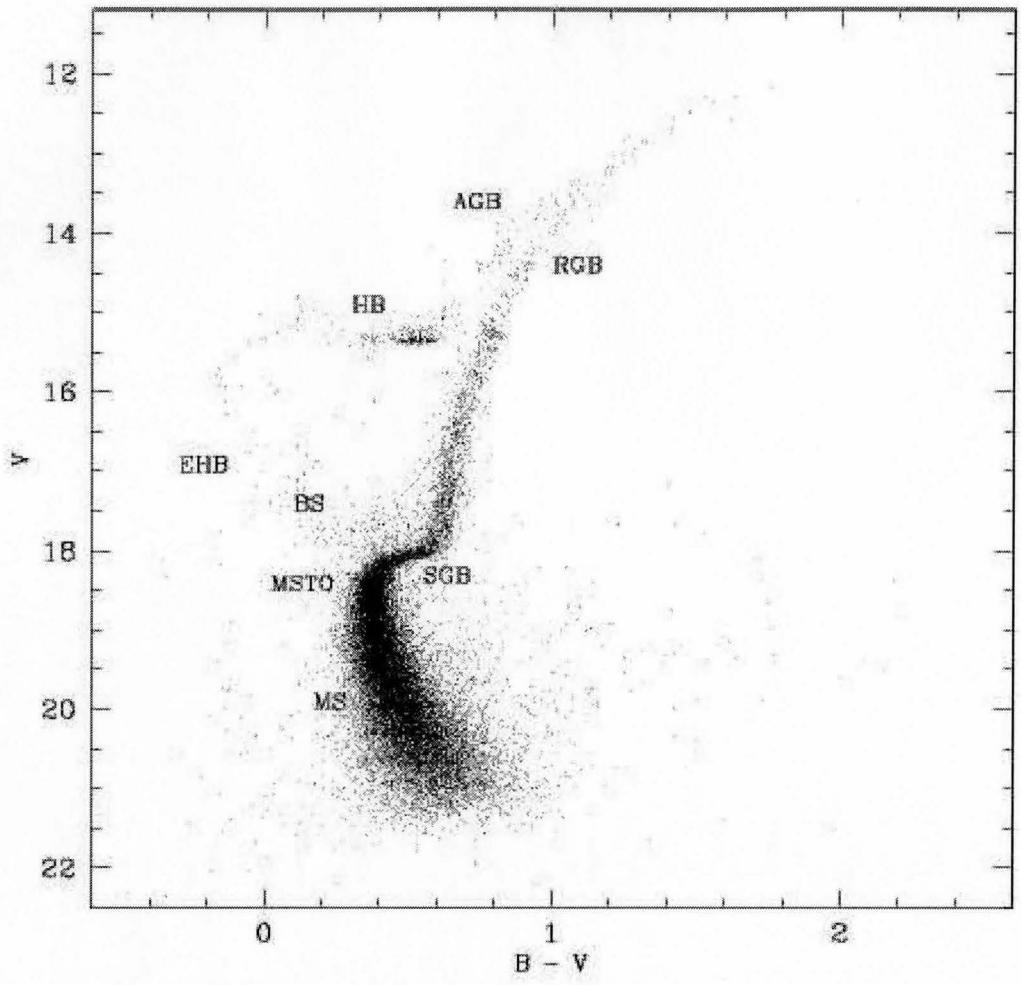

Figure 1.1: Colour-magnitude diagram for the globular cluster NGC 362. Each of the main phases of stellar evolution are shown: the main sequence (MS); blue stragglers (BS); the main-sequence turn-off point (MSTO); the sub-giant branch (SGB) or hydrogen shell-burning phase; the red giant branch (RGB) or phase prior to helium core-burning; the horizontal branch or helium core-burning phase (HB); the asymptotic giant branch or hydrogen and helium shell-burning phase; the extended horizontal branch (EHB). The data used to make this plot was taken from Piotto et al. (2002).

from looking solely at the internal mechanics of stars to that of the entire cluster in which they reside, it seems likely that most stars do not evolve in isolation at all, but rather interact in a complex dance carefully choreographed by gravity that could very well influence their observable traits. Exactly how stars interact over the course of a cluster's lifetime is a function of numerous factors and while we cannot predict the precise evolution, it seems likely that its destiny depends on the nature of its internal machinery (e.g. Binney & Tremaine, 1987).

Clusters can ultimately be categorized according to a variety of different parameters including density, total mass, age, and binary fraction. Despite a continuum of possible combinations of these parameters, two broad categories of cluster can be defined: globular and open (or galactic). Globular clusters (GCs) are typically very old, having ages on the order of 10^{10} years (Binney & Tremaine, 1987). Their open counterparts, on the other hand, display a range of ages, from about 10^{6} to around 10^{10} years (Binney & Tremaine, 1987). Open clusters (OCs) are much more sparsely populated than globular clusters, with numbers ranging from a dozen to as many as a few million members. Since they are more dynamically evolved, GCs (as well as older OCs) tend to be more compact and are characterized by an overall symmetric shape, while younger OCs tend to look more like their parent nebulae (Fregeau et al., 2002). Different cluster environments are likely to stimulate different dynamical processes at different rates. For instance, one might expect binary mergers to occur with greater frequency in clusters having a high binary fraction. It is for this reason that the dynamical history of clusters may also play an important role in understanding the trends exhibited in CMDs (Hut et al., 2003).

1.2 A Brief Introduction to Blue Stragglers

Blue straggler stars (BSSs) could be clues to the complex machinery of stellar populations. They represent the inability of stellar evolution alone in isolated single star systems to explain the observed trends in temperature and luminosity that stars generally adhere to. Discovered by Sandage (1953) in the cluster M3, BSSs are brighter and bluer (hotter) than the cluster MSTO, having seemingly neglected to make the transition to lower effective temperatures along with the rest of the cluster population. Despite numerous formation mechanisms having been proposed over the years, a satisfactory explanation as to how exactly these stars are created eludes us still. Do they represent an extended period of star formation within the cluster? Are they the result of a prolonged main-sequence (MS) lifetime due to internal mixing? And what of the possibility of stars actually interacting, or even merging, within a cluster? The currently favoured answer, while poorly defined, is thought to depend on the cluster dynamics. The notion of somehow forming stars that are more massive than the present MSTO mass to explain the existence of BSSs is one that has persisted. There is a growing consensus that these stars are the products of stellar mergers between two (or possibly more) low mass MS stars, whether it be through collisional processes or the coalescence of a primordial binary system (Leonard, 1989; Livio, 1993; Stryker, 1993; Bailyn, 1995). In order for a binary system to coalesce, Roche lobe overflow must occur, triggering the onset of mass transfer from the outer envelope of an evolved donor onto that of its companion (McCrea, 1964). Primordial binary coalescence is, as such, dependent on the donor star's evolutionary state since the process is governed by how tenuously gravity is holding onto its atmosphere, in addition to the

degree of orbital separation. Collisions, on the other hand, do not depend as much on the evolutionary status of the participants since in this case, two (or more) stars pass very close to one another, form a brief and highly eccentric binary system, and then rapidly spiral inwards and merge as tidal interactions dissipate energy (Leonard, 1989). Hence, it is generally thought that coalescence requires relative isolation from surrounding stars and should occur on a much longer timescale than do collisions. There is evidence to suggest that both formation mechanisms are occurring and it seems as though the preferred creation pathway is dependent on the cluster environment (e.g. Warren et al., 2006). It may, as such, be useful to consider the dynamical interactions preferentially occurring in different environments separately.

Blue stragglers provide strong evidence in favor of the notion that stars do not evolve in complete isolation over the course of their lives. Rather, it is thought that they interact in various ways and that such dynamical processes can have a pronounced impact on observations. In order to gain a complete understanding of the general trends we see in CMDs, we need to combine our knowledge of stellar evolution with what we currently know regarding stellar dynamics. Additionally, we must consider and put into context the evolution of entire stellar populations in order to be able to integrate a given cluster's history into a cohesive understanding of the observations. Clearly, if dynamical processes are indeed a factor in producing the stellar populations that we see, then knowing a cluster's history can prove a crucial ingredient in explaining the data.

1.3 Thesis Objectives

No clear correlation has as of yet been established between BSS formation and environment. The literature contains a great deal of conflicting information on the subject, suggesting that multiple creation pathways may be needed to explain the origins of these exotic stars. If this is the case, then one might expect that the preferred mode of formation should depend on the cluster dynamics. The primary aim of this M.Sc. thesis was to ascertain the environmental conditions under which either collisions or coalescence would most likely occur.

Chapter 2 describes some of the more important studies that focused on BSSs, including a description of previous attempts at distinguishing them from other stars in a CMD. A set of BSS selection criteria are defined in Chapter 3 as well as a set of criteria for identifying RGB stars and for distinguishing between the HB and the EHB. Relative BSS frequencies were found for each cluster using the RGB, the HB, the EHB, or both the HB & the EHB for normalization and have been plotted against several cluster parameters for comparison, including total mass (total cluster magnitude), age, central density, and central velocity dispersion. In Chapter 4, the relevant dynamical processes and concepts pertaining to globular cluster evolution are explained and are related to BSS production. Chapter 5 outlines a crude model we have created in an attempt to reproduce the observations, in addition to some preliminary results and a brief discussion. Finally, Chapter 6 provides a summary of the results.

Bibliography

Bailyn, C. D. 1995, ARA&A, 33, 133

Binney, J. & Merrifield, M. 1998, Galactic astronomy (Princeton, NJ, Princeton University Press)

Binney, J. & Tremaine, S. 1987, Galactic dynamics (Princeton, NJ, Princeton University Press)

Carroll, B. W. & Ostlie, D. A. 2006, An introduction to modern astrophysics (2nd edition. San Francisco: Pearson, Addison-Wesley)

Fregeau, J. M., Joshi, K. J., Portegies Zwart, S. F., & Rasio, F. A. 2002, ApJ, 570, 171

Hut, P., Shara, M. M., Aarseth, S. J., Klessen, R. S., Lombardi, Jr., J. C., Makino, J., McMillan, S., Pols, O. R., Teuben, P. J., & Webbink, R. F. 2003, New Astronomy, 8, 337

Leonard, P. J. T. 1989, AJ, 98, 217

Livio, M. 1993, in ASP Conf. Ser. 53: Blue Stragglers, ed. R. A. Saffer, 3

McCrea, W. H. 1964, MNRAS, 128, 147

Piotto, G., King, I. R., Djorgovski, S. G., Sosin, C., Zoccali, M., Saviane, I., De Angeli, F., Riello, M., Recio-Blanco, A., Rich, R. M., Meylan, G., & Renzini, A. 2002, A&A, 391, 945

Sandage, A. R. 1953, AJ, 58, 61

Sills, A. & Bailyn, C. D. 1999, ApJ, 513, 428

Stryker, L. L. 1993, PASP, 105, 1081

Warren, S. R., Sandquist, E. L., & Bolte, M. 2006, ApJ, 648, 1026

Chapter 2

A History of Blue Stragglers

2.1 Cluster Dynamics

A host of dynamical processes are thought to occur in dense stellar populations, though there is still some debate as to which of them occur with the highest efficiency and the greatest frequency in the presence of particular environmental conditions. It is thought that the majority of stars in the dense cores of GCs experience the dynamical effects of collisions, most notably in clusters for which the stellar collision time is comparable to the cluster lifetime (Hills & Day, 1976). While we cannot see these encounters take place directly, observational evidence for stellar interactions comes in the form of peculiar binary systems. For instance, cataclysmic variables (CVs), exceptionally tight binary systems characterized by mass transfer via Roche lobe overflow from a MS (or sometimes RGB) star onto a white dwarf companion, have been directly detected in numerous clusters including NGC 6752 (Bailyn et al., 1996) and NGC 6397 (Cool et al., 1996).

Low-mass X-ray binaries (LMXBs) have been observed to display oscillations in brightness orders of magnitude more rapid than in CVs and are thought to be the result of a similar mass transfer process between MS or RGB stars and neutron stars (Kaaret et al., 2004) or black holes (McClintock, 2004). LMXBs tend to form via either tidal capture or three-body exchange collisions. In the latter case, a NS or a BH encounters a regular binary system and, due to its intense gravitational influence, the compact object can cause the least massive star to be ejected from the system, thus creating a new binary pair with a compact object as one of its members (Hills & Day, 1976). Tidal capture, on the other hand, occurs when a compact object experiences a grazing collision with a single ordinary star, warping its shape and ultimately facilitating capture as energy is released from the system when the regular star is subjected to the intense tidal forces of the NS or BH (Baumgardt et al., 2006). Compact objects are thought to replace one of the members of primordial binary systems with enough frequency to account for the abundance of millisecond pulsars and X-ray binaries found in GC cores (Rasio et al., 2000).

Interactions between stars can have important implications for the dynamical evolution of a cluster. Core collapse, through the use of analytic models and numerical simulations, has been shown to be driven by the dissipation of kinetic energy via tidal encounters, mass segregation, and the gravothermal instability, through which the most massive stars force the collapse in a very short time by means of collisions and mergers (Spitzer, 1987). In the first 10^7 years of a cluster's life, a runaway collapse of the core can occur due to collisional processes and mergers, which can in turn fuel the formation of a massive central object if the stars have not had enough time to evolve and die

in supernovae explosions (Gürkan et al., 2004). On the other hand, if these massive stars have had sufficient time to die, the collapse of the core will stop and can even be reversed due to the mass loss triggered by supernovae, which provide a source of heating in the core by accelerating nearby stars. In this case, the result will be a cluster containing numerous stellar-mass black holes (BHs). In smaller systems such as globular clusters, however, it is generally thought that most of these BHs will be ejected from the core as a result of 3-body and 4-body interactions (Mapelli et al., 2004).

Cluster cores tend to be significantly different morphologically and dynamically than their halos. Observations from the Hubble Space Telescope (HST) suggest that BSSs are primarily located in the cores of GCs (Ferraro et al., 1999), though they have also been detected in their outskirts. The BSS populations have been found to have a bimodal distribution with radius in clusters like M55 (Zaggia et al., 1995), M3 (Ferraro et al., 1997), and 47 Tuc (NGC 104) (Ferraro et al., 2004), with elevated numbers in the cores that fall off temporarily and then rise again in the clusters' outer regions. While the source of the gap remains unknown, this bimodal trend seems indicative of two separate formation mechanisms dominating in the core and in the field, with mass transfer primarily taking place in the outer regions and collisions mainly occurring towards the cluster center. In the case of M3, however, this bimodal distribution has been speculated to primarily be the result of collisional processes occurring in the core, from which BSSs get ejected into the outer regions of the cluster due to conservation of momentum or recoil from impact (Sigurdsson et al., 1994).

2.2 Observational Evidence for BSS Formation

Eclipsing binaries consisting of MS components having short periods and sharing a common envelope, called contact or W UMa binaries, have been observed among BSSs in sparse globular (Mateo et al., 1990; Yan & Mateo, 1994) and open clusters (Ahumada & Lapasset, 1995). The discovery of these systems is strong evidence that blue stragglers form in binary systems. Meanwhile, HST observations have revealed significant numbers of BSSs within the dense cores of globular clusters, hinting at the prudence of not discounting collisional processes to explain the origin of BSSs (de Marchi & Paresce, 1994); (Ferraro et al., 1999). Complicating matters further still, it has been suggested that collisions need not only occur between two single stars in exceptionally dense environments, but could also occur in less dense systems when primordial binaries interact resonantly so that the orbits of both binary systems become significantly perturbed by the interaction (Bacon et al., 1996). Such interactions can actually increase the collision rate when two primordial binary systems remain tightly gravitationally bound since the probability of experiencing a close encounter or collision between any two of the four stars increases dramatically (Fregeau et al., 2004). There are many possible ways in which multiple stellar systems might interact with one another and it is conceivable that more than one of them could offer a practical explanation of the BSS phenomenon. In fact, multiple collisions between stars are thought to be responsible for some of the blue stragglers that we see, in particular those having masses around twice that of our Sun or more (Sepinsky et al., 2000).

The degree of mixing that takes place in a merger event is a key consideration in predicting the location of the remnant in the CMD. If added helium is mixed into the outer layers, the star will appear brighter and bluer than it otherwise would. For the most part, mixing is thought to take place in collision products, most notably in the core where added hydrogen can be dumped, prolonging the MS lifetime of the merger remnant (Benz & Hills 1987; 1992). Using stellar evolution models, Sills et al. (1995) found that the observed characteristics of 6 bright BSSs in the core of NGC 6397 could only be explained by evolving models that were initially mixed. Conversely, significantly less mixing is generally expected to take place during the much slower process of binary coalescence, occurring on an evolutionary rather than a dynamical timescale (Bailyn, 1992). Since collisional products are thought to undergo more mixing and so have helium-enriched outer layers relative to mass-transfer products, the possibility of merger remnants forming via different means being observationally distinguishable may be plausible, though the concept remains controversial (Bailyn, 1992); (Sills et al., 1995).

There is growing evidence that the more massive a cluster, the lower the frequency of BSSs. Recently, Piotto et al. (2004) examined the CMDs of 56 different GCs, comparing the frequencies of BSSs to cluster properties like total mass (absolute luminosity) and central density. The relative frequencies were approximated by normalizing the number of BSSs to the HB or RGB (the results did not depend on which specific frequency they chose). They found that the higher the mass of the cluster, the smaller the relative frequency of BSSs, suggesting that the preferred formation mechanism may depend on the cluster mass.

2.3 Which ones are the Blue Stragglers?

Colour-magnitude diagrams are often so cluttered that distinguishing the blue stragglers from ordinary MSTO stars, or even those belonging to the horizontal (HB) and extended horizontal branches (EHB), can be a challenging task. In looking at the BSS populations of 6 different GCs, Ferraro et al. (1997) defined boundaries to separate the BSSs from regular MS stars in an ultraviolet CMD. Using the brightest portion of the HB for normalization, they shifted the CMD of each cluster to coincide with that of M3 for consistency and then divided the blue straggler population into two separate sub-samples: bright BSSs with $m_{255} < 19$ mag and faint BSSs with $19.0 < m_{255} < 19.4$ mag. Figure 2.1 shows the CMDs in the (m_{255} - m_{336}, m_{255})-plane for 6 clusters with the BSS selection boundaries overlaid.

Recently, de Marchi et al. (2006) looked at 216 OCs containing a total of 2105 BSS candidates in order to compare the blue straggler frequency to the cluster mass (total magnitude) and age. Using a more conventional (B - V, V)-plane, they found an anti-correlation between BSS frequency and total magnitude, extending the results of Piotto et al. (2004) to the open cluster regime. They also found a good correlation between the BSS frequency and the cluster age, suggesting that at least one of the formation mechanisms requires a long timescale to operate with any appreciable frequency. In an attempt to be consistent in their analysis, de Marchi et al. defined their own criteria for the selection of blue stragglers. Contrary to Ferraro et al. (1997), they defined

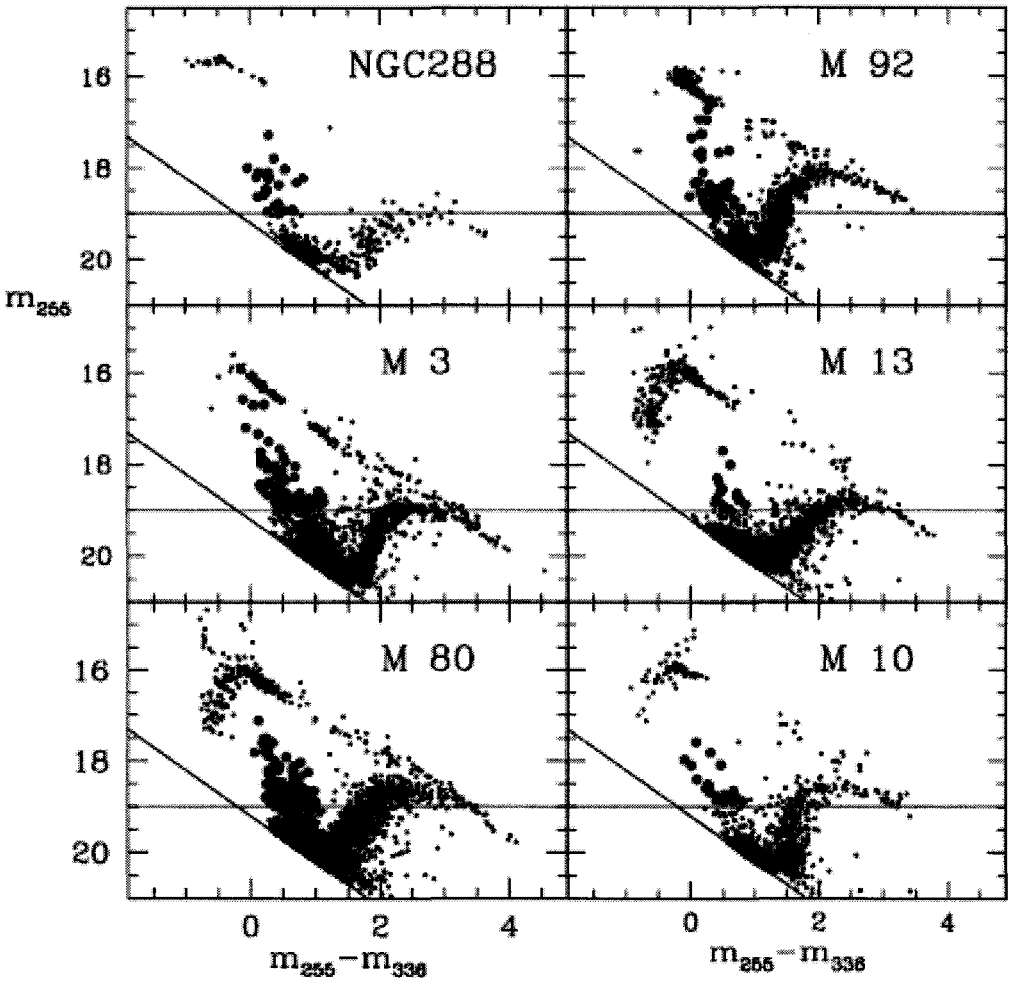

Figure 2.1: CMDs for the indicated clusters in the $(m_{255} - m_{336}, m_{255})$-plane. Each CMD has been appropriately shifted to coincide with that of M3, for which the horizontal line corresponds to $m_{255} = 19$. The large circles represent the bright BSS candidates (taken from Figure 1 of Ferraro et al. (2003)).

their boundaries by drawing a line twice as bright (as indicated by the 'B' subscript) as the zero-age main sequence:

$$V_{Bi} = V_i - 0.75 \tag{2.1}$$

$$(B-V)_{Bi} = (B-V)_i \tag{2.2}$$

and then placed two borders as follows ('l' stands for left or a shift to bluer colours and 'r' stands for right or a shift to redder colours):

$$V_{li} = V_i + \Delta V \tag{2.3}$$

$$(B-V)_{li} = (B-V)_i - \Delta(B-V) \tag{2.4}$$

$$V_{ri} = V_{Bi} - \Delta V \tag{2.5}$$

$$(B-V)_{ri} = (B-V)_{Bi} + \Delta(B-V), \tag{2.6}$$

where ΔV and $\Delta(B-V)$ are arbitrarily set to 0.15 mag in order to account for differential reddening and photometric errors. Figure 2.2 below shows how these boundary conditions are applied to the open cluster NGC 7789.

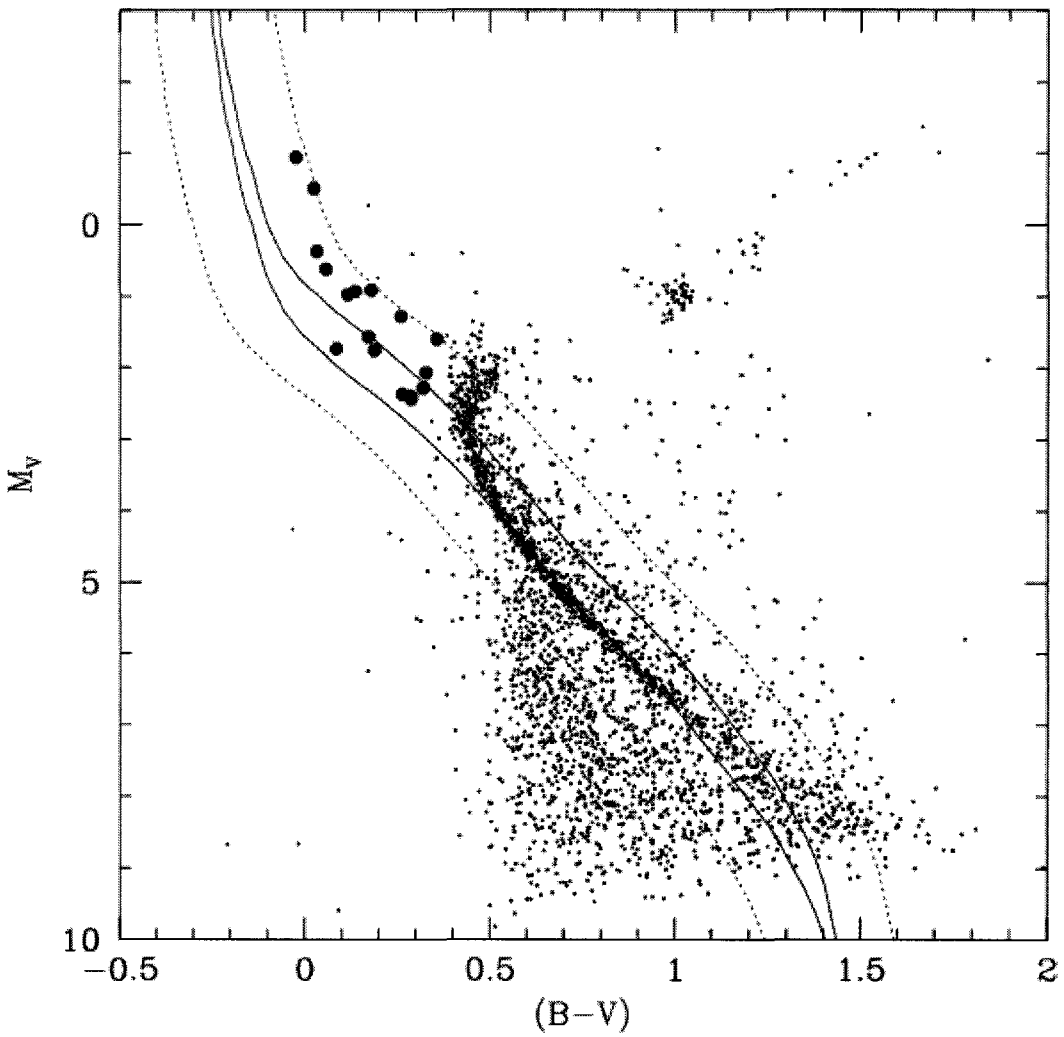

Figure 2.2: CMD for the open cluster NGC 7789 in the (B-V,V)-plane. The filled-in circles represent BSS candidates. Solid lines represent the theoretical ZAMS for single stars and for binaries with equal mass components. The dashed lines depict the aforementioned sequences shifted by 0.15 mag in B-V and in V in order to properly account for photometric error and differential reddening (taken from Figure 1 of de Marchi et al. (2006)).

Bibliography

Ahumada, J. & Lapasset, E. 1995, A&AS, 109, 375

Bacon, D., Sigurdsson, S., & Davies, M. B. 1996, MNRAS, 281, 830

Bailyn, C. D. 1992, ApJ, 392, 519

Bailyn, C. D., Rubenstein, E. P., Slavin, S. D., Cohn, H., Lugger, P., Cool, A. M., & Grindlay, J. E. 1996, ApJ, 473, L31

Baumgardt, H., Hopman, C., Portegies Zwart, S., & Makino, J. 2006, MNRAS, 372, 467

Cool, A. M., Sosin, C., King, I. R., Cohn, H. N., Lugger, P. M., Bailyn, C. D., & Grindlay, J. E. 1996, Bulletin of the American Astronomical Society, 28, 1371

de Marchi, F., de Angeli, F., Piotto, G., Carraro, G., & Davies, M. B. 2006, A&A, 459, 489

de Marchi, G. & Paresce, F. 1994, ApJ, 422, 597

Ferraro, F. R., Beccari, G., Rood, R. T., Bellazzini, M., Sills, A., & Sabbi, E. 2004, ApJ, 603, 127

Ferraro, F. R., Paltrinieri, B., Fusi Pecci, F., Cacciari, C., Dorman, B., Rood, R. T., Buonanno, R., Corsi, C. E., Burgarella, D., & Laget, M. 1997, A&A, 324, 915

Ferraro, F. R., Paltrinieri, B., Rood, R. T., & Dorman, B. 1999, ApJ, 522, 983

Ferraro, F. R., Sills, A., Rood, R. T., Paltrinieri, B., & Buonanno, R. 2003, ApJ, 588, 464

Fregeau, J. M., Cheung, P., Portegies Zwart, S. F., & Rasio, F. A. 2004, MNRAS, 352, 1

Gürkan, M. A., Freitag, M., & Rasio, F. A. 2004, ApJ, 604, 632

Hills, J. G. & Day, C. A. 1976, Astrophys. Lett., 17, 87

Kaaret, P., Lamb, F. K., & Swank, J. H., eds. 2004, American Institute of Physics Conference Series, Vol. 714, X-Ray Timing 2003: Rossi and Beyond

Mapelli, M., Sigurdsson, S., Colpi, M., Ferraro, F. R., Possenti, A., Rood, R. T., Sills, A., & Beccari, G. 2004, ApJ, 605, L29

Mateo, M., Harris, H. C., Nemec, J., & Olszewski, E. W. 1990, AJ, 100, 469

McClintock, J. 2004, APS Meeting Abstracts, D3004

Piotto, G., De Angeli, F., King, I. R., Djorgovski, S. G., Bono, G., Cassisi, S., Meylan, G., Recio-Blanco, A., Rich, R. M., & Davies, M. B. 2004, ApJ, 604, L109

Rasio, F. A., Pfahl, E. D., & Rappaport, S. 2000, ApJ, 532, L47

Sepinsky, J. F., Saffer, R. A., Pilman, C. S., DeMarchi, G., & Paresce, F. 2000, Bulletin of the American Astronomical Society, 32, 740

Sigurdsson, S., Davies, M. B., & Bolte, M. 1994, ApJ, 431, L115

Sills, A., Bailyn, C. D., & Demarque, P. 1995, ApJ, 455, L163

Spitzer, L. 1987, Dynamical evolution of globular clusters (Princeton, NJ, Princeton University Press)

Yan, L. & Mateo, M. 1994, AJ, 108, 1810

Zaggia, S. R., Piotto, G., & Capaccioli, M. 1995, in IAU Symp. 164: Stellar Populations, ed. P. C. van der Kruit & G. Gilmore, 409

Chapter 3

Relative BSS Frequencies and Cluster Environment[1]

In this Chapter we define a series of BSS selection rules to obtain relative BSS frequencies for comparison with global cluster parameters. Observational implications pertaining to blue straggler formation mechanisms are then discussed and suggestions for modeling globular cluster dynamics are presented.

3.1 The Database

The colour-magnitude diagrams and photometric databases for 74 Galactic globular clusters were used in this thesis. The observations, taken from Piotto et al. (2002), were made using the HST's WFPC2 camera in the F439W and F555W bands, with the PC camera centered on the cluster center in each case. Generally, the field of view for each cluster contains anywhere from a few thousand to roughly 47,000 stars. Of the 74 potential GGCs, only 57 were

[1] Much of this chapter has already been published as Leigh, N., Sills, A., & Knigge, C. Where the Blue Stragglers Roam: Searching for a Link Between Formation and Environment, ApJ, accepted, 2007.

deemed fit for analysis, with the remaining 17 having been discarded due to poor reliability of the data at or above the main sequence turnoff. The positions of the stars, as well as their magnitudes in both the F439W and F555W bands and the B and V standard Johnson system, can be found at the Padova Globular Cluster Group Web pages at http://dipastro.pd.astro.it/globulars.

The data available at the Padova website have not been corrected for completeness. This is only likely to be a problem if we cannot accurately determine the total number of blue stragglers, horizontal branch, extended horizontal branch, and red giant stars. However, we do not expect this to be an issue in this M. Sc. thesis. All of the chosen clusters in our sample have readily identifiable main sequence turnoffs and sub-giant branches. BS, HB, EHB, and RGB stars are all, by definition, brighter than the turnoff and should consequently be less affected by photometric errors and completeness. Since the sample size is small, we expect that the corrections for the faintest blue stragglers in our sample should be on the order of one star or less for each cluster, which will have a negligible impact on the results of this M. Sc. thesis. However, to be prudent, stars having sufficiently large errors in m_{555} and m_{439}, respectively denoted by σ_{F555W} and σ_{F439W}, were also rejected from the counts if their total error exceeded 0.1 magnitudes.

3.2 Blue Straggler Selection Criteria

We defined a set of boundaries in the colour-magnitude diagram for each of the populations of interest: blue stragglers, red giant branch stars, horizontal branch stars, and extended horizontal branch stars. The boundary conditions

were ultimately chosen for consistency. By eliminating potential selection effects such as "by eye" estimates, we were able to minimize the possibility of counting EHB or MSTO stars as BSSs. Moreover, since we are considering relative frequencies and there is a possibility of mistakenly including stars other than BSSs in our counts, it seems prudent that we at least make the attempt to systematically choose stars in all clusters. We are most interested in using the evolved populations to normalize the number of blue stragglers, both to give a sense of photometric error and to remove the predictable trend that clusters with more stars have more BSSs. Therefore, we limited ourselves to red giants with the same luminosities as the blue stragglers.

We chose to take as our starting point the sharpest point in the bend of the MSTO centered on the mass of points that populate it (denoted by $((B-V)_0, V_0)$). From here, we defined a "MSTO width", w, in the $m_{439}-m_{555}$ plane to describe its approximate thickness, and then established a second reference point, $(B-V, V)$, by shifting $w/4$ mag bluer in $m_{439}-m_{555}$ and $5w/8$ bluer in m_{555}, as indicated in Equation 3.1:

$$B - V = (B-V)_0 - w/4 \tag{3.1}$$

$$V = V_0 - 5w/8 \tag{3.2}$$

This "by eye" shift ensured that our boundary selection starting point, namely the outer edge of the MSTO, was nearly identical for every cluster. In order to separate the BSSs from the rest of the stars that populate the region just above the MSTO, we drew two lines of slope -3.5 in the $(m_{439}-m_{555}, m_{555})$-plane made to intersect points shifted from $(B-V, V)$. One line was shifted 0.5 mag bluer in $m_{439}-m_{555}$ and 0.1 mag bluer in m_{555} from $(B-V, V)$,

whereas the other was shifted 2.0 mag bluer in $m_{439} - m_{555}$ and 0.4 mag bluer in m_{555}. These new points of intersection are shown in Equation 3.3 below:

$$(B-V)_r = (B-V) - 0.5 \tag{3.3}$$

$$V_r = V - 0.1 \tag{3.4}$$

$$(B-V)_l = (B-V) - 2.0 \tag{3.5}$$

$$V_l = V - 0.4 \tag{3.6}$$

Two further boundary conditions were defined by fitting two lines of slope 5.0, chosen to be more or less parallel to the fitted ZAMS, one intersecting a point shifted 0.2 mag redder in $m_{439} - m_{555}$ and 0.5 mag bluer in m_{555} from $(B-V, V)$ (top), and another passing through a point 0.2 mag bluer in $m_{439} - m_{555}$ and 0.5 mag redder in m_{555} (bottom). These new intersection points are given by:

$$(B-V)_{t,b} = (B-V) \pm 0.2 \tag{3.7}$$

$$V_{t,b} = V \mp 0.5 \tag{3.8}$$

These cuts eliminate obvious outliers and further distinguish BSSs from HB and EHB stars. The methodology used in de Marchi et al. (2006) for isolating BSSs similarly incorporated the ZAMS, though their upper and lower boundaries were ultimately defined differently, as outlined in Chapter 2. Finally, one last cut was made to distinguish BSSs from the EHB, namely a vertical one made 0.4 mag bluer in $m_{439} - m_{555}$ than the MSTO. Refer to Figure 3.1 for an example of how the aforementioned boundary conditions are applied.

3.3 RGB Selection Criteria

A similar methodology was used to isolate the RGB stars in the cluster CMDs. We are restricting ourselves to RGB stars in the same magnitude range as the blue straggler stars. First, two lines of slope -19.0 in the $(m_{439} - m_{555}, m_{555})$-plane were drawn to intersect the MSTO. In order to place them on either side of the RGB, both lines were shifted 0.6 mag bluer in m_{555} though it was necessary to apply different colour shifts. The left-most boundary was placed 0.15 mag redder in $m_{439} - m_{555}$ while the right-most boundary was placed 0.45 mag redder in $m_{439} - m_{555}$. To fully define our RGB sample, a lower boundary was defined using a horizontal cut made 0.6 mag above the MSTO (lower in m_{555}). The upper boundary, on the other hand, was simply defined to be the lower boundary of the HB. RGB stars must therefore simultaneously satisfy (see Figure 3.1):

$$-19.0(B-V)_{RGB} + (V - 0.6) + 19.0((B-V) + 0.15) < V_{RGB} \tag{3.9}$$

$$V_{RGB} < -19.0(B-V)_{RGB} + (V - 0.6) + 19.0((B-V) + 0.45) \tag{3.10}$$

$$V - 0.6 < V_{RGB} \tag{3.11}$$

$$V_{RGB} > h + 0.4 \tag{3.12}$$

3.4 HB and EHB Selection Criteria

Pulling out HB and EHB stars from the cluster CMDs was found to be more difficult than for BSSs and RGB stars due to the awkward shape of the bend as the HB extends down to lower luminosities. Exactly where the HB

ends and the EHB begins has always been a matter of some controversy, and so the choice of where to place the boundary was arbitrary but was at least consistent from cluster to cluster.

A vertical boundary was placed 0.5 mag bluer in $m_{439} - m_{555}$ than the MSTO to distinguish the end of the HB from the start of the EHB. The center-most part (in absolute magnitude) of the grouping of stars that make up the HB, denoted by h, was carefully chosen by eye, and two horizontal borders were subsequently defined 0.4 mag above and below. One more boundary, this time a vertical cut to help distinguish the HB from the RGB, was set 0.3, 0.4, or 0.5 mag redder in $m_{439} - m_{555}$ than the MSTO. The decision of which of these three HB_{shift}'s to use was decided for each cluster based on their individual CMDs. Every star in the CMD that fell to the left of this vertical boundary and in between the horizontal ones was taken to be an HB star, and every star that was not already counted as a BSS or a member of the HB was then taken to be an EHB star. Thus, HB stars, denoted by $((B-V)_{HB}, V_{HB})$, must simultaneously satisfy (see Figure 3.1):

$$(B-V)_{HB} < (B-V) + HB_{shift} \tag{3.13}$$

$$h - 0.4 < V_{HB} < h + 0.4 \tag{3.14}$$

Finally, it was necessary to eliminate any very faint EHB stars to avoid including any white dwarfs in our sample. Hence, a final boundary was set 3.5 mag below the lower boundary of the HB. This then implies that EHB stars, denoted by $((B-V)_{EHB}, V_{EHB})$, must satisfy:

$$(B-V)_{EHB} < (B-V) - 0.5 \tag{3.15}$$

$$h + 0.4 < V_{EHB} < h + 0.4 + 3.5 \tag{3.16}$$

One small region of concern for the EHB remains undefined in the CMDs, namely the portion just above the "left" BSS boundary with slope -3.5 that also falls to the right of our vertical EHB/BSS dividing line and below the lower HB boundary. For simplicity, we treat these stars as belonging to the EHB, though note that our frequencies would not have been altered by much had we taken them to be BSSs, and even less so had we taken them to be HB stars. As such, in addition to the above criteria, EHB stars can also simultaneously satisfy:

$$(B - V)_{EHB} > (B - V) - 0.5 \tag{3.17}$$

$$V_{EHB} > h + 0.4 \tag{3.18}$$

$$V_{EHB} < -3.5(B - V)_{EHB} + (V - 2.0) + 3.5((B - V) - 0.4) \tag{3.19}$$

In Table 3.1, we give the cluster name, the number of BSS, HB, EHB, RGB, and core stars, as well as parameters needed to make these selections: the width of the main sequence w, the position of the MSTO, and the level of the horizontal branch.

Table 3.1: Population Selection Criteria and Numbers

NGC	$N_{BSS/HB/EHB/RGB}$	N_{core}	w	$(B\text{-}V)_{MSTO}$	V_{MSTO}	V_{HB}
0104	35/200/ 2/648	28924	0.150	0.510	17.100	13.800
0362	41/118/ 14/343	20359	0.140	0.390	18.300	15.200
1261	6/ 21/ 1/ 51	9265	0.220	0.410	19.600	16.700

continued on next page

NGC	$N_{BSS/HB/EHB/RGB}$	N_{core}	w	$(B\text{-}V)_{MSTO}$	V_{MSTO}	V_{HB}
1851	13/ 43/ 5/117	21923	0.200	0.480	18.900	16.000
1904	25/ 23/ 54/238	14485	0.200	0.450	19.500	16.000
2808	47/212/132/975	46328	0.250	0.400	18.700	15.500
3201	14/ 20/ 2/ 83	3175	0.200	0.530	17.100	14.100
4147	16/ 14/ 7/ 53	2675	0.180	0.400	20.000	16.900
4372	11/ 11/ 7/ 95	1847	0.170	0.430	17.700	14.500
4590	24/ 30/ 2/180	5253	0.150	0.380	18.800	15.500
4833	20/ 50/ 51/300	6461	0.180	0.400	17.800	14.500
5024	28/ 69/ 85/421	12997	0.250	0.370	20.000	16.700
5634	27/ 54/ 44/252	6868	0.300	0.350	20.800	17.500
5694	17/ 5/133/184	14914	0.290	0.460	21.300	17.800
4499	23/ 46/ 1/186	3221	0.250	0.390	20.100	16.900
5824	34/ 52/139/233	28046	0.310	0.400	21.100	18.000
5904	16/ 69/ 38/270	14696	0.190	0.410	18.100	15.000
5927	33/117/ 1/324	15856	0.300	0.630	18.700	15.200
5946	1/ 7/ 49/ 89	7032	0.310	0.520	19.000	15.500
5986	21/ 68/150/588	16141	0.210	0.430	18.900	15.600
6093	27/ 22/132/356	11390	0.300	0.520	18.800	15.400
6171	14/ 24/ 3/ 93	2972	0.220	0.670	17.900	14.600
6205	14/ 25/168/735	13276	0.300	0.430	18.300	14.700
6229	38/ 86/ 79/385	8999	0.330	0.450	21.100	18.000

continued on next page

NGC	$N_{BSS/HB/EHB/RGB}$	N_{core}	w	$(B-V)_{MSTO}$	V_{MSTO}	V_{HB}
6218	26/ 5/ 34/166	5142	0.170	0.480	17.500	13.900
6235	7/ 3/ 22/106	3288	0.230	0.420	19.100	15.500
6266	24/ 76/ 80/483	21369	0.300	0.510	17.900	14.700
6273	32/ 21/178/715	32692	0.310	0.490	18.300	15.000
6284	4/ 11/ 28/ 74	7890	0.220	0.500	19.600	16.400
6287	14/ 25/ 26/132	4827	0.300	0.520	18.700	15.400
6293	5/ 5/ 24/ 52	16707	0.180	0.370	18.400	15.200
6304	15/ 51/ 2/162	11524	0.230	0.580	18.000	14.600
6342	7/ 8/ 0/ 34	4809	0.310	0.590	18.800	15.400
6356	23/187/ 2/565	18223	0.320	0.580	20.000	16.500
6362	23/ 37/ 2/161	4084	0.160	0.510	18.500	14.900
6388	64/479/ 54/1054	46933	0.500	0.590	19.100	15.700
6402	19/181/145/445	12347	0.380	0.510	18.700	15.400
6397	4/ 0/ 4/ 3	16507	0.100	0.370	15.700	12.500
6522	0/ 3/ 5/ 28	16426	0.210	0.490	18.600	15.100
6544	3/ 0/ 2/ 8	3196	0.230	0.530	16.300	12.700
6584	22/ 51/ 3/291	5679	0.220	0.400	19.500	16.100
6624	15/ 25/ 0/104	12537	0.300	0.580	18.600	15.200
6638	18/ 51/ 5/238	6737	0.250	0.530	18.900	15.500
6637	20/ 82/ 1/294	8523	0.260	0.570	18.800	15.400
6642	14/ 26/ 1/ 56	2938	0.200	0.510	18.600	15.200

continued on next page

NGC	$N_{BSS/HB/EHB/RGB}$	N_{core}	w	$(B\text{-}V)_{MSTO}$	V_{MSTO}	V_{HB}
6652	14/ 16/ 4/ 64	5749	0.150	0.560	19.000	15.600
6681	4/ 2/ 4/ 24	6056	0.170	0.450	18.800	15.400
6712	39/ 64/ 3/294	9540	0.250	0.500	18.100	14.800
6717	10/ 3/ 1/ 17	1623	0.220	0.470	18.500	15.400
6723	14/ 72/ 25/290	7052	0.180	0.510	18.600	15.300
6838	17/ 9/ 3/ 56	2132	0.150	0.570	17.000	13.800
6864	27/165/ 14/391	10132	0.230	0.440	20.200	17.200
6934	18/ 56/ 11/201	9472	0.190	0.430	19.700	16.600
6981	18/ 50/ 1/149	5704	0.170	0.390	19.800	16.800
7078	10/ 47/ 32/223	32581	0.210	0.380	18.600	15.500
7089	5/ 28/ 69/244	11723	0.190	0.390	19.000	15.500
7099	10/ 8/ 56/ 30	8010	0.200	0.380	18.300	15.000

As mentioned, all of the aforementioned boundary conditions are shown in Figure 3.1.

3.5 Results

3.5.1 Considerations Regarding the Core and the Geometrical Scaling Factor

The data obtained by Piotto et al. (2002) comes from HST/WFPC2 observations, with the PC camera centered on the cluster center in each case. This made distinguishing stars within a core radius a relatively straightfor-

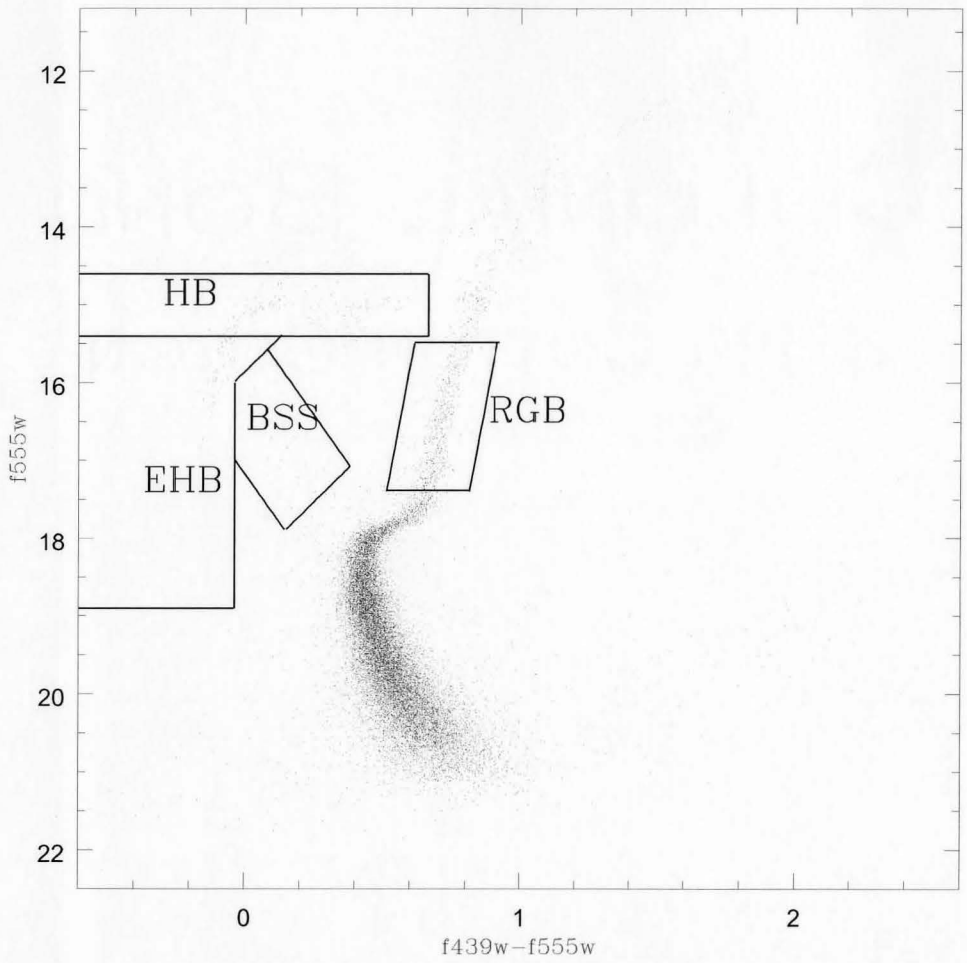

Figure 3.1: CMD for the cluster NGC 5904 with BS, RGB, HB, and EHB boundaries overlaid. Data was taken from (Piotto et al., 2002).

ward process. In order for our counts to be representative of the entire core, however, it was necessary to extrapolate our results in the case of clusters for which only a fraction of the core was sampled. Therefore, the total number of stars found in each cluster was multiplied by the ratio of the entire core area to that of the sampled region.

Since the data was normalized to allow for an accurate comparison of the BSS cluster populations, amending our BSS, RGB, HB, and EHB counts in this way would not have had an effect on the relative frequencies. That is, when considering only those stars within the core or only those stars outside, the geometrical correction factor cancels out upon normalization. The scaling factor was ultimately added for consistency so that we were analyzing the total number of core stars, as opposed to a different fraction thereof, for each cluster. A consistent count of the total number of core stars was necessary for calculating some of the parameters used for comparison in this study.

After calculating separate relative BSS frequencies inside and outside the cluster core as well as for the entire field of view, we decided to focus solely on those stars found within the core. Our reasoning was twofold. First, we felt it more or less realistic to assume an approximately uniform core as far as the stellar density and distribution were concerned. Recently, Ferraro et al. (1997) discovered that M3 has a bimodal blue straggler distribution with a clear "zone of avoidance" separating the inner and outer populations. It seems feasible then that the core blue straggler population is predominantly a product of a single formation mechanism operating in an approximately uniform environment. Second, our goal was to create a consistent sampling from cluster

to cluster. Since BSSs are thought to be a dynamically-created population, it seemed wise to focus on a specific portion of the cluster that is home to a more or less uniform dynamical environment. Since the core is small compared to the rest of the cluster, interactions between stars occur with roughly the same frequency everywhere therein. Consequently, not much of a dynamical gradient is thought to exist within one core radius.

3.5.2 Methods of Normalization

With our sample of BS, HB, EHB, and RGB stars established consistently from cluster to cluster, it was then necessary to address the issue of normalization. As one might expect, clusters having more stars tend to be home to a larger population of BSSs, as is shown in Figure 3.2.

It therefore proved necessary to normalize the data in order to properly account for this trend, and so number counts of stars had to be converted into relative BSS frequencies. Previously, this was done by dividing the number of BSSs by either the number of horizontal branch stars (Piotto et al., 2004):

$$F_{BSS}^{HB} = \frac{N_{BSS}}{N_{HB}}, \tag{3.20}$$

or by the total cluster mass (de Marchi et al., 2006):

$$F_{BSS}^{M_{tot}} = \frac{N_{BSS}}{M_{tot}} \tag{3.21}$$

The preferred means of normalization is a matter of some debate and hence the relative frequencies were calculated in a few separate ways in order to gauge

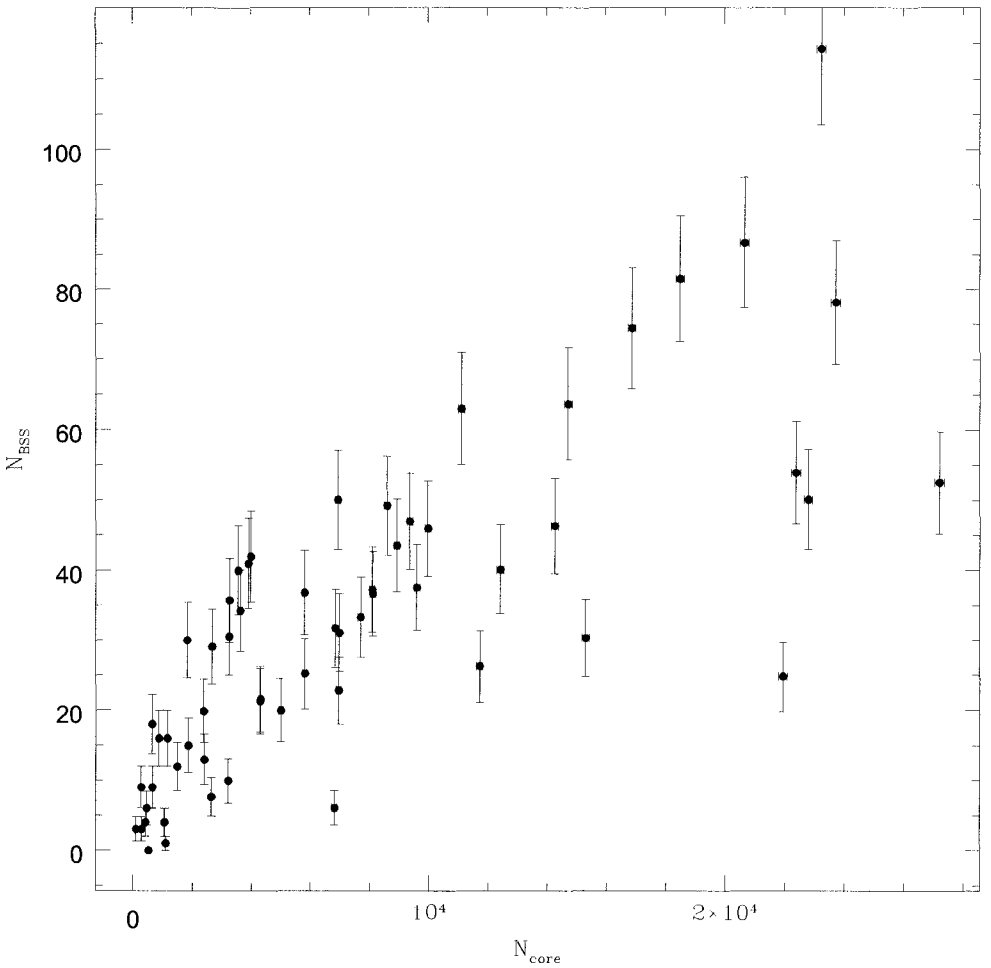

Figure 3.2: Plot of the number of BS stars within the cluster core versus the total number of stars (prior to factoring in the geometrical scaling factor) therein.

which is best. Frequencies were normalized using the HB, the EHB, the HB & the EHB, and the RGB:

$$F_{BSS}^{HB} = \frac{N_{BSS}}{N_{HB}} \tag{3.22}$$

$$F_{BSS}^{EHB} = \frac{N_{BSS}}{N_{EHB}} \tag{3.23}$$

$$F_{BSS}^{HB+EHB} = \frac{N_{BSS}}{N_{HB} + N_{EHB}} \tag{3.24}$$

$$F_{BSS}^{RGB} = \frac{N_{BSS}}{N_{RGB}} \tag{3.25}$$

Plotting the frequencies against the total cluster mass (or total V magnitude), previously shown by Piotto et al. (2004) to exhibit a clear anti-correlation, proved that using either the HB or the EHB alone for normalization tended to produce more scatter in the plots than using both together. Many clusters have both a sparsely populated HB and a well-represented EHB, hence combining HB and EHB stars for normalization should primarily reduce F_{BSS} in HB-poor clusters, minimizing scatter in our plots. Furthermore, plots normalized using only EHB stars tended to have significantly more scatter than those normalized using the HB alone. Using the RGB, however, gives us the tightest relationship. This reduction of scatter was similarly observed upon comparing the BSS frequency to other cluster parameters like the central surface brightness, the central velocity dispersion, as well as the collisional rate. Figure 3.3 shows the BSS frequency versus the total absolute V magnitude of the cluster for all four normalization methods.

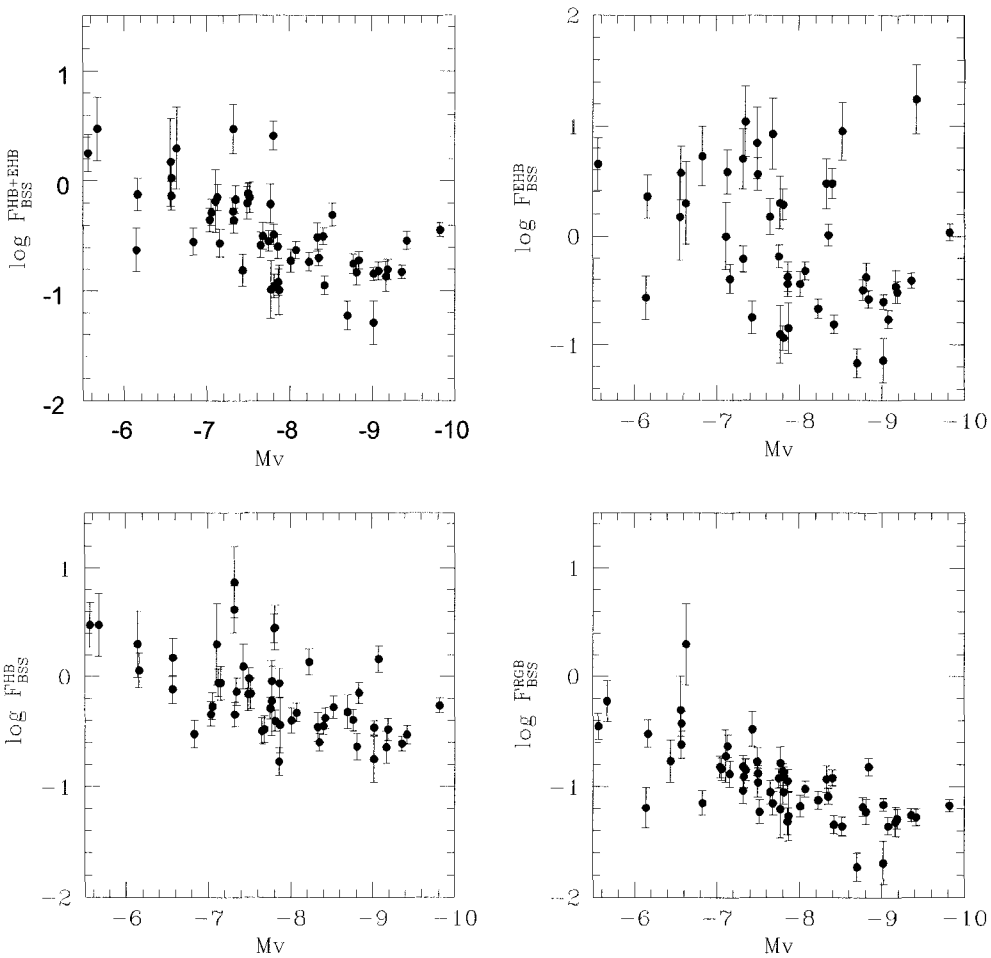

Figure 3.3: Plots of the core BSS frequency versus the total cluster V magnitude. Frequencies were normalized using RGB stars (bottom right), HB stars (bottom left), EHB stars (top right), and finally, HB & EHB stars combined (top left).

3.5.3 Relating Relative BSS Frequencies to Cluster Parameters

Having obtained the numbers and frequencies of blue stragglers in the cluster cores, we attempted to determine correlations between the blue straggler frequency and global cluster properties such as total mass, velocity dispersion, core density, etc. If the preferred BSS formation mechanism in the core is collisions, then we should see a link between clusters with a higher frequency of collisions and the BSS population; if the preferred mode of formation is not collisions, however, we should still look for a relationship between BSS populations and global cluster properties.

The central surface brightness and the core radius were taken from Harris (1996). Values for the central velocity dispersion were taken from Pryor & Meylan (1993). All other parameters, including the central density and the total absolute luminosity, came from Piotto et al. (2002), with the exception of the normalized cluster ages which were taken from De Angeli et al. (2005) and for which the Zinn & West (1984) metallicity scale values were employed. Error bars for all plots were calculated assuming Poisson statistics.

It should be noted that while the number of blue straggler stars in the core is a tracer of the total number of stars therein, as well as of the total number of HB and RGB stars, we found no correlation between the number of blue stragglers and the number of EHB stars. It has been speculated (Ferraro et al., 2003) that there might be a connection between BSS and EHB populations. The trend in that paper (of 6 clusters) was that clusters either had bright blue stragglers or EHB stars, but not both. We do not find the same result with our

bigger self-consistent sample. The number of EHB stars seems to be entirely independent of the number of bright blue stragglers populating the cluster.

Relative frequencies appeared independent of the majority of the cluster parameters analyzed, with a couple of noteworthy exceptions. One apparent trend observed was that the least massive clusters (those having the lowest absolute luminosities) had the highest relative frequency of blue stragglers, and vice versa. This anti-correlation was similarly seen by Piotto et al. (2004), though their choice of BSS selection and method of normalization arguably led to more scatter in their plots. They also did not distinguish between blue stragglers inside or outside of one core radius but simply counted the stars in their observed fields.

A similar anti-correlation was found between F_{BSS} and the central velocity dispersion, shown in Figure 3.4. This is perhaps unsurprising, since velocity dispersion is known to be correlated with cluster mass (Djorgovski & Meylan, 1994). The blue straggler frequencies showed no clear dependence on any other cluster parameters, including the central density, the central surface brightness, and the cluster age.

Figure 3.5 shows the blue straggler frequency versus the core and half-mass relaxation times. In general, the term relaxation time describes the exchange of gravitational energy that occurs in a cluster to define its density and velocity distributions. The more relaxation times a cluster undergoes, the more dynamically evolved it becomes. While weak anti-correlations were found with both the core and half-mass relaxation times, F_{BSS} was found to show a stronger anti-correlation with the latter. Moreover, it seems as though the

distribution begins to flatten out at higher log t_h, specifically beyond around 10^9 years.

We also considered the brightest blue stragglers (BBSSs) separately, under the assumption that these stars are most likely to be collision products. Figure 2 of Monkman et al. (2006) shows that, in the case of 47 Tuc (NGC 104), the number of bright blue stragglers falls off noticeably outside the cluster core. These brightest blue stragglers found only within the core have a B magnitude of less than about 15.60 mag, or a V magnitude of less than about 15.36 mag. Assuming the BBSSs in other clusters are similar to the ones found in 47 Tuc, we defined the brightest BSSs as those having a V magnitude of 1.74 mag brighter than that of the MSTO. As illustrated in Figure 3.6, the usual trends with M_V and the central velocity dispersion were found. No new trends between the BBSS relative frequencies and any cluster parameters emerged.

We also looked at the relative BSS frequencies in only the most massive clusters for which $M_V < -8.8$ under the assumption of Davies et al. (2004) that the BSSs in these clusters should predominantly be collision products. Collisional BSSs are thought to be brighter than those formed from primordial binaries. As illustrated in Figure 3.7, no trends were found between BSS relative frequencies and any cluster parameters when clusters with $M_V > -8.8$ were ignored. Indeed, the previously established trend between M_v and F_{BSS} is considerably weakened by eliminating clusters with $M_V > -8.8$.

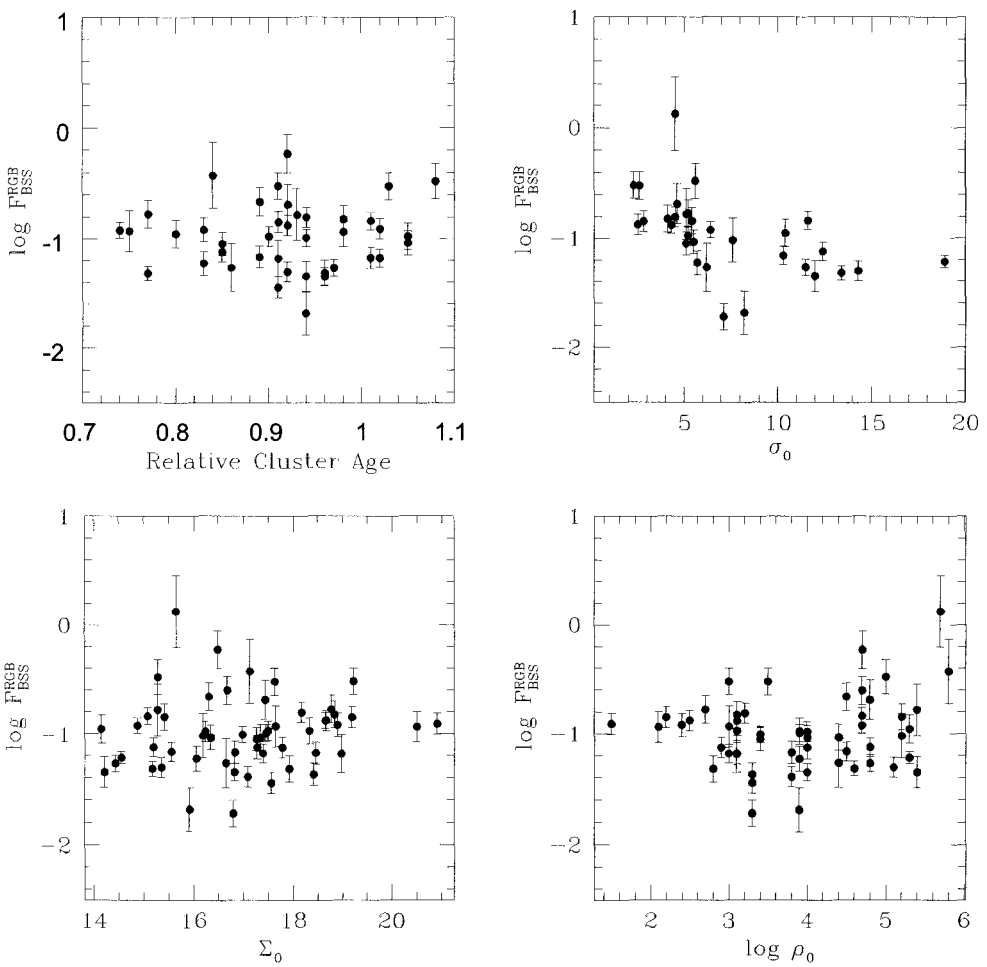

Figure 3.4: Plots of the core BSS frequency versus the logarithm of the central density (bottom right), the central surface brightness (bottom left), the relative cluster age (top left), and the central velocity dispersion (top right). Frequencies were normalized using RGB stars. The central density is given in units of $L_\odot$ pc^{-3}, the central surface brightness in units of V mag arc $second^{-2}$, and the central velocity dispersion in units of km s^{-1}. The relative cluster age represents the ratio between the actual cluster age and the mean age of a group of metal-poor clusters (11.2 Gyrs), as described in De Angeli et al. (2005).

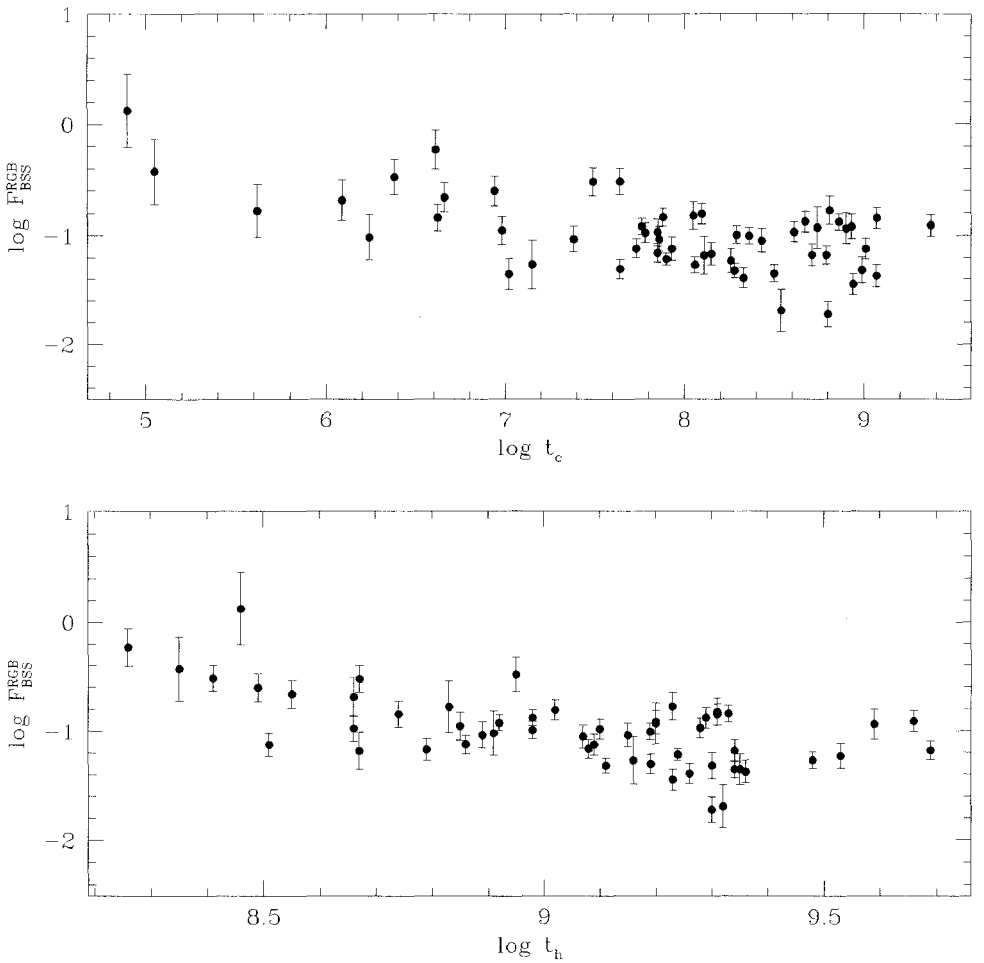

Figure 3.5: Plots of the core BSS frequency versus the logarithm of the core relaxation time in years (top), and the logarithm of the relaxation time at the half-mass radius in years (bottom). Frequencies were normalized using RGB stars. Note the weak anti-correlation that exists between F_{BSS} and log t_h.

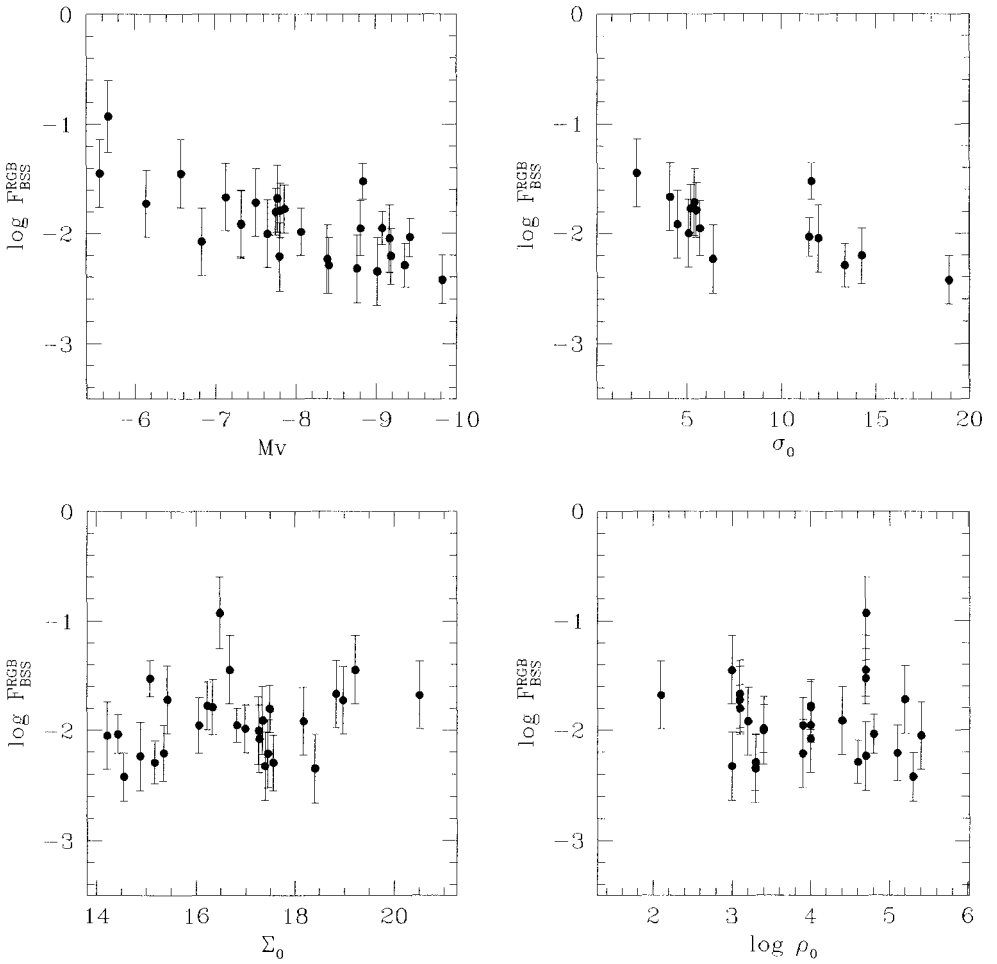

Figure 3.6: Plots of the brightest core BSS frequency versus the logarithm of the central density (bottom right), the central surface brightness (bottom left), the total cluster V magnitude (top left), and the central velocity dispersion (top right). Frequencies were normalized using RGB stars. The central density is given in units of $L_\odot$ pc^{-3}, the central surface brightness in units of V mag arc $second^{-2}$, the cluster magnitude in V mag, and the central velocity dispersion in units of km s^{-1}.

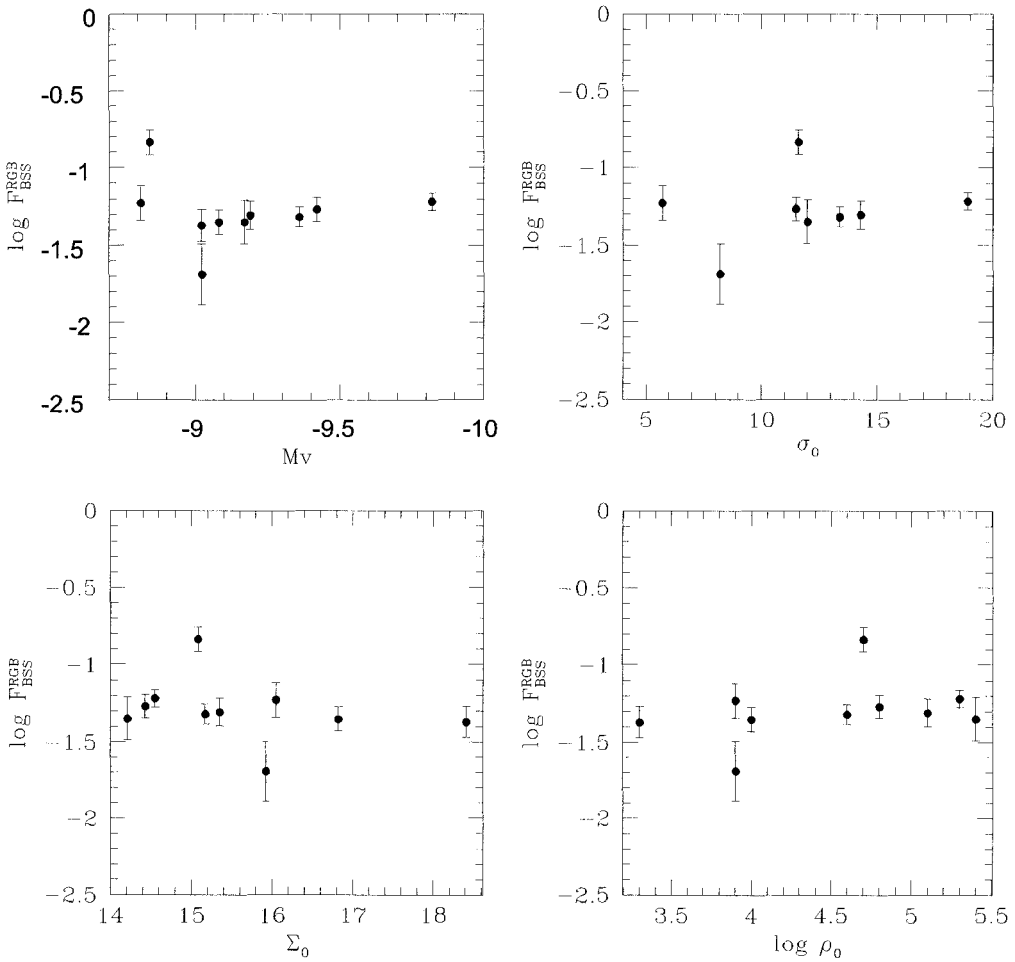

Figure 3.7: Plots of the core BSS frequency in only the brightest clusters ($M_V < -8.8$) versus the logarithm of the central density (bottom right), the central surface brightness (bottom left), the total cluster V magnitude (top left), and the central velocity dispersion (top right). Frequencies were normalized using RGB stars. The central density is given in units of $L_\odot$ pc^{-3}, the central surface brightness in units of V mag arc $second^{-2}$, the cluster magnitude in V mag, and the central velocity dispersion in units of km s^{-1}.

3.5.4 Collisional Parameters

BSS frequencies were also plotted against two parameters used to approximate the rate of stellar collisions per year. The first such parameter is given by (Piotto et al., 2004):

$$\Gamma_1 = 5.0 \times 10^{-15} (\Sigma_0^3 r_c)^{1/2}, \tag{3.26}$$

where Σ_0 is the central surface brightness in units of $L_{\odot,V}$ pc^{-2} and r_c is the radius of the cluster core in parsecs. Equation 3.26 was derived for a King model GC and so it is assumed that the most energetic stars will have been removed by the galaxy's tidal influence. The second collisional parameter is given by (Pooley & Hut, 2006):

$$\Gamma_2 = \frac{\rho_0^2 r_c^3}{\sigma_0}, \tag{3.27}$$

where ρ_0 is the central density in units of $L_{\odot,V}$ pc^{-3}, σ_0 is the central velocity dispersion in km s^{-1} and r_c is again the core radius in parsecs.

If there is a tight correlation between the fraction of blue stragglers and Γ, then we can conclude that direct stellar collisions are responsible for most of the blue stragglers in cluster cores. Figure 3.8 and Figure 3.9 show, if anything, a decline in BSS frequency with increasing collisional rate. These possible weak anti-correlations are likely not an artifact of the more populous clusters having more stars available to undergo collisions since we are dealing with normalized BSS frequencies as opposed to pure number counts. This anti-correlation has been seen by Piotto et al. (2004) and Sandquist (2005) for blue straggler populations belonging to a larger portion of the cluster. The trend is weak, and one could argue that there is no correlation.

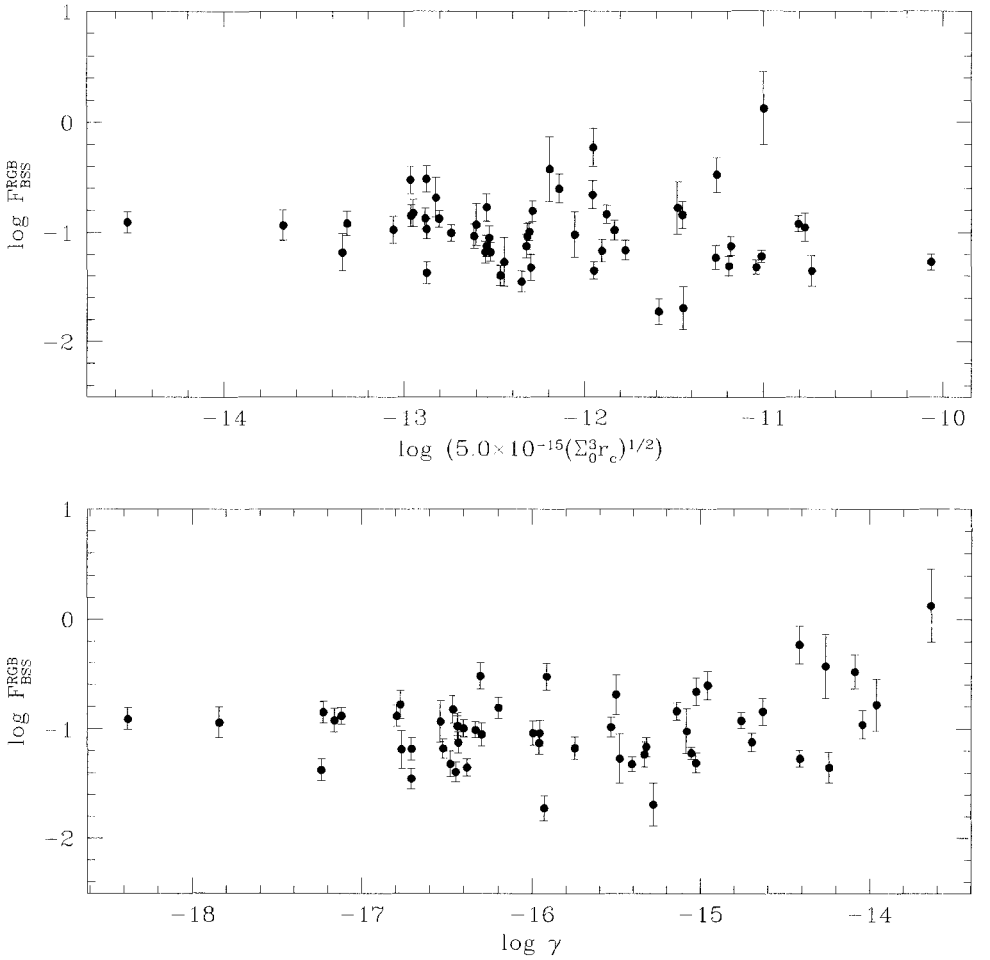

Figure 3.8: Plot of the BSS frequency within the cluster core versus the rate of stellar collisions (number of collisions per year) occurring within the core per year using Equation 3.26 as the collisional parameter (top). BSS frequency is also plotted against the probability of a stellar collision occurring within the core in one year (bottom). Σ_0 is the central surface brightness in units of $L_\odot$ pc^{-2} and r_c is the core radius in parsecs. Frequencies were normalized using core RGB stars.

An additional comparison can be made to the probability that a given star will undergo a collision in one year, denoted by γ. We divide the rate of stellar collisions by the total number of stars in the cluster core, $N_{\rm star}$, found by directly counting them in Piotto et al.'s (2002) database and then multiplying by the appropriate geometrical correction factor. In order for our counts to be representative of the entire core, it was necessary to extrapolate our results in the case of clusters for which only a fraction of the core was sampled, as described in Section 3.5. Figure 3.9 and Figure 3.8 clearly show that there is no dependence of F_{BSS} on γ. We also looked for connections between both Γ and γ and the brightest blue stragglers, and the blue stragglers in the brightest clusters. We found no trends in either case.

If real, the weak dependence of F_{BSS} on the collisional rates is evidence in support of collisional processes being an important factor in blue straggler formation, albeit one that operates to impede their production rather than enhance it. We had expected to see F_{BSS} increase with increasing Γ, since intuitively one would expect a higher incidence of collisions to generate more BSSs. This was, however, not the case.

A possible contribution to the observed weak anti-correlation between Γ and F_{BSS} pertains to the average BSS mass for each cluster. Clusters having a higher collisional rate should undergo more collisions and, as such, are more likely to undergo more high-order collisions. As a result, those clusters having the highest values for Γ and surprisingly low values for F_{BSS} are potentially home to a greater abundance of blue stragglers formed via three- or possibly even four-body collisions. Thus, if higher order collisions occur preferentially

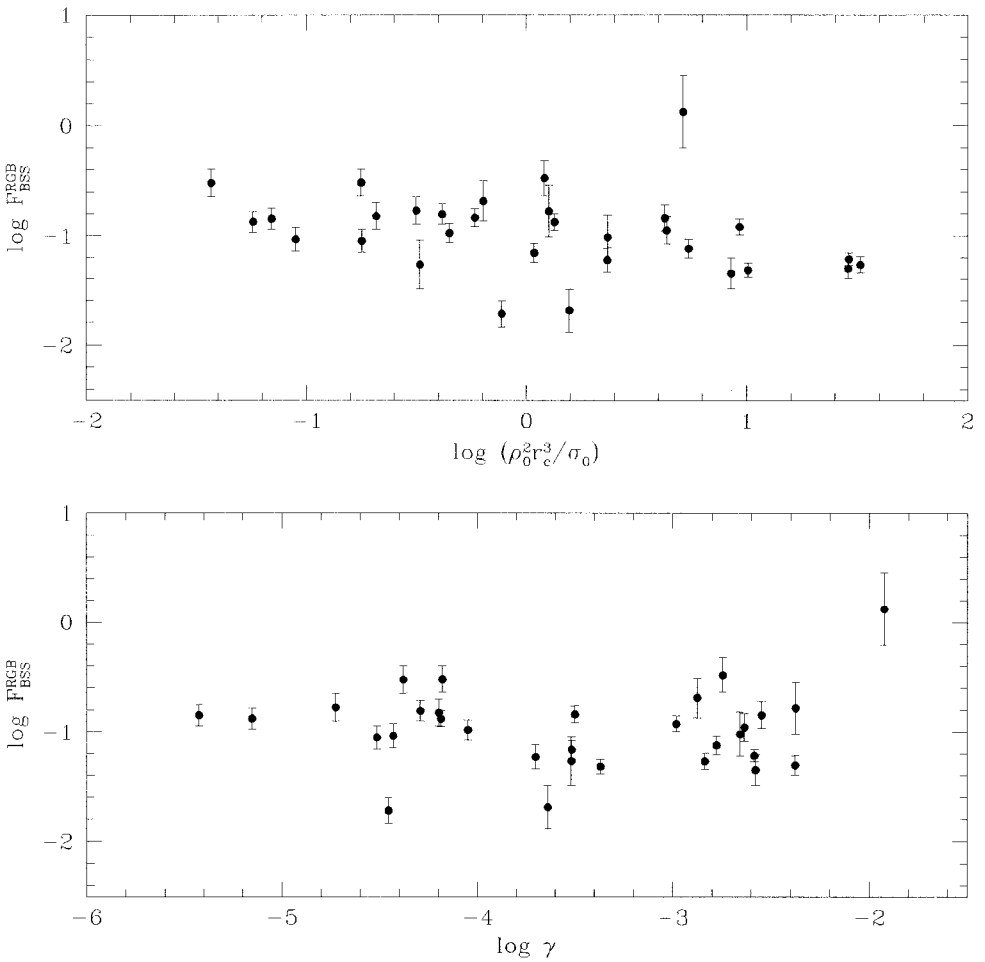

Figure 3.9: Plot of the BSS frequency within the cluster core versus the rate of stellar collisions per year using Equation 3.27 as the collisional parameter (top). Note that Equation 3.27 provides a relative estimate for the frequency of collisions and that the units do not directly provide the number of collisions per year. BSS frequency is also plotted against the probability of a stellar collision occurring within the core in one year (bottom). ρ_0 is the central density in units of $L_\odot$ pc^{-3}, σ_0 is the central velocity dispersion in km s^{-1}, and r_c is the core radius in parsecs. Frequencies were normalized using core RGB stars.

in certain clusters then the BSSs produced therein could be, on average, more massive than in less collisionally-affected environments, contributing to a lower observed F_{BSS}. This effect is not seen, however, in the blue straggler luminosity functions (BSLFs) and is, as such, expected to play only a small role in the outcome of F_{BSS}.

3.5.5 Error Analysis

To quantify these dependencies, or lack thereof, we have calculated the Spearman correlation coefficients (Press et al., 1992) between the blue straggler frequency and a variety of cluster parameters. Spearman's rank coefficient, r_s, provides a measure of correlation and assesses the degree to which some monotonic function describes the relationship between two variables without making any a priori assumptions regarding the frequency distribution of the variables. Raw scores in the data are converted to ranks and the difference between the ranks of each data point, $X_i - Y_i$, are calculated. r_s is given by:

$$r_s = 1 - 6\frac{(X_i - Y_i)^2}{N(N^2 - 1)}, \tag{3.28}$$

where N is the number of data points.

The results of this analysis are given in Table 3.2. The correlation coefficient r_s ranges from 0 (no correlation) to 1 (completely correlated), or to -1 (completely anti-correlated). The third column, labeled "Probability", gives the chance that these data are uncorrelated. Clearly the most important anti-correlations are with the total cluster magnitude and the central velocity dispersion (the Spearman coefficient for M_V is positive for an anti-correlation

Table 3.2: Spearman Correlation Coefficients

Parameter	r_s	Probability
Total cluster V magnitude	0.76	7.2E-12
Central velocity dispersion	-0.70	1.0E-05
Half-mass relaxation time	-0.53	2.5E-05
Core relaxation time	-0.43	1.1E-03
Collision Rate	-0.41	0.02
Surface Brightness	0.17	0.20
Central density	0.08	0.58
Collision probability	-0.09	0.63
Age	0.02	0.91

because the magnitude scale is backwards). The anti-correlation with half-mass relaxation time also shows up here, and the frequency of blue stragglers in clusters may also be anti-correlated with the core relaxation time and collision rate, although this is not conclusive from these data.

3.5.6 Luminosity Functions

Having investigated the relationship between the frequency of blue stragglers and their host cluster properties, we now turn to looking at the details of the blue straggler population itself. Cumulative blue straggler luminosity functions (BSLFs) were made for all 57 clusters in our sample. The magnitude of the MSTO differs from cluster to cluster and so, in order to correct for these discrepancies, it was subtracted from the BSS magnitudes in each cluster.

We wanted to quantify the shape of these luminosity functions in order to determine if there were any connections between BSLF shape and global cluster parameters. We found that all the BSLFs could be well-fit using a

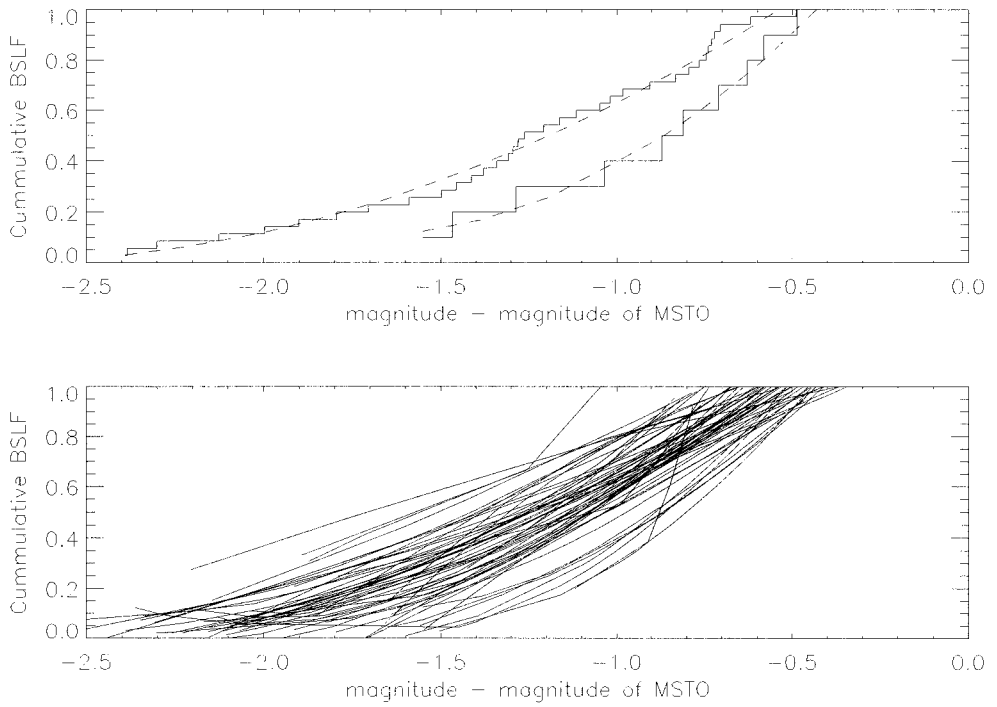

Figure 3.10: Cumulative BS luminosity functions. The top panel shows the BSLFs for NGC 104 (47 Tucanae) and NGC 7099 (M30) (solid lines) along with quadratic fits to those functions (dashed lines). The bottom panel shows the quadratic fits to all cluster BSLFs.

quadratic (but not a linear) function of magnitude. Some examples of the fits are given in the top panel of Figure 3.10. The fits for all clusters are given in the bottom panel.

We looked at each of the quadratic coefficients as a function of all of the cluster parameters, and found that the coefficients had no dependency on any parameter, including total cluster magnitude or metallicity. We were particularly interested in metallicity since the BSLF is a measure of the properties of BSS stellar evolution, which could depend on metallicity. According to these data, it does not.

Piotto et al. (2004) argued that if the BSS formation mechanisms depend on the cluster mass, then one would expect the blue straggler LFs to likewise depend on the mass. They predicted that the luminosity distribution of collisionally produced BSSs should differ from those created via mass transfer or the merger of a binary system due to different resulting interior chemical profiles. They were able to generate separate BSLFs for clusters with $M_V < -8.8$ and $M_V > -8.8$ in support of their hypothesis. Upon subtracting MSTO magnitudes from peak BSLF magnitudes and creating individual BSLFs for clusters above and below a total V magnitude of -8.8, we found the difference between the two sub-sets of BSLFs to be negligible. Interestingly, there were in total only 11 clusters in our data set for which $M_V < -8.8$ and so, had we found any potential trends, their reliability would be suspect. Any generalizations made regarding the most massive clusters should be disregarded due to the small number of clusters in the Piotto et al. (2002) data-set in this regime.

We repeated this experiment by binning our BSLFs according to cluster magnitude, in bins of size 1 magnitude. The results are shown in Figure 3.11. We see no trend in the peak of the BSLF with cluster magnitude. We also tried binning the BSLFs by central density (in bins of size 1 in $\log \rho_0$) and by half-mass relaxation time (in bins of size 0.5 in $\log t_h$). Again, we found no trend in the peak magnitude or shape of the luminosity function for any of these parameters. We expect, given our analysis of the shapes of the cumulative BSLFs, that binning by any other cluster parameter will similarly yield no trends. Just to check, we performed a Kolmogorov-Smirnov test on the luminosity functions that were binned by absolute cluster magnitude (those shown in Figure 3.11). No pairs of distributions were drawn from the same

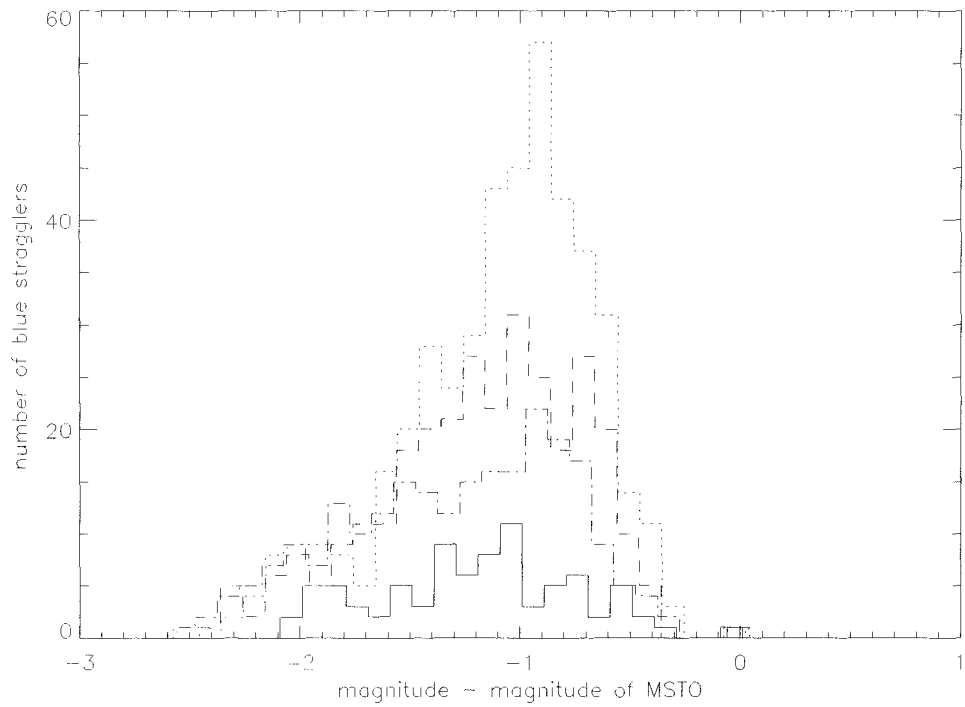

Figure 3.11: Blue straggler luminosity functions, binned according to total cluster magnitude. The solid line is for clusters with M_V between -6 and -7; dotted line for clusters with M_V between -7 and -8; dashed line for clusters with M_V between -8 and -9, and the dash-dotted line is for clusters with M_V between -9 and -10.

parent distribution with more than a few percent probability. The closest pair ($-7 < M_V < -6$ and $-9 < M_V < -8$) have a 57% probability of being drawn from the same distribution; and all other pairs were below the 10% level.

3.6 Summary and Discussion of Observational Results

We used the large homogeneous database of HST globular cluster photometry from Piotto et al. (2004) to investigate correlations of blue stragglers with

their host cluster properties. First, we applied a consistent definition of "blue straggler" to all our clusters. We chose the MSTO as our starting point and defined our boundaries based only on its location in the CMD. We also defined the location of horizontal branch and extended horizontal branch stars in the CMD. We looked at a variety of normalizations for our BSS frequencies before determining that using the RGB yielded the plots with the least scatter.

There are disappointingly few strong correlations between the frequency of blue stragglers in the cores of these clusters and any global cluster parameter. We confirm the anti-correlation between the the total integrated cluster luminosity and relative BSS frequency found by Piotto et al. (2004); we suggest an anti-correlation with central velocity dispersion based on a high correlation coefficient comparable to that found for the cluster luminosity. At a lower significance are possible anti-correlations with half-mass and core relaxation times.

The relaxation time for a cluster is a measure of how long a system can live before individual stellar encounters become important and the approximation of objects moving in a smooth mean potential breaks down. Globular clusters are the quintessential collisional dynamical systems, since their ages are typically much longer than their relaxation times. It seems sensible that the fraction of blue stragglers, a dynamically created population, should depend on the relaxation times of clusters. The puzzle comes, as usual, in the details. First, we are looking at core blue stragglers, so we might expect the blue straggler fraction to go up with decreasing core relaxation time. The observations do give us this kind of trend, but not a very strong one. We might also expect

the blue straggler fraction to depend on the half-mass relaxation time, which is a better measure of the dynamical state of the whole system. The blue straggler fraction does depend on t_h in the way that we expect, but only for systems with short dynamical times. Is blue straggler formation a dynamical process which takes a while to turn on? It seems that might be the case.

If the observed anti-correlation between F_{BSS} and the central velocity dispersion is real, then it follows that random relative motions somehow impede stellar mergers. A similar conclusion can be drawn from the plots of F_{BSS} versus Γ in the event that the speculated anti-correlations are truly representative of the cluster dynamics. Collisional processes therefore seem to somehow interfere with the production of BSSs. If the majority of BSSs are, in fact, the remnants of coalescing binaries then it stands to reason that an increase in the number of close encounters or collisions with other stars could result in the disruption of a larger number of binary systems. On the other hand, if the majority of BSSs are the products of stellar collisions, then it is conceivable that those clusters having the highest collisional frequencies are the most likely to undergo three- or four-body encounters. As such, clusters having the highest collisional rates could also have, on average, the most massive BSSs resulting from an increased incidence of multi-body mergers. This might then contribute to the observed weak anti-correlation between F_{BSS} and the collisional rate since clusters having a higher incidence of collisions should consequently have a higher incidence of multi-body mergers, resulting in a potentially lower relative BSS frequency. We need more, and more accurate, individual surface gravity measurements of blue stragglers in order to explore the idea that a surplus of more massive BSSs can be found in those clusters with a higher Γ.

F_{BSS} was found to be nearly uniform with every other cluster parameter, suggesting that all globular clusters of all properties produce the same fraction of blue stragglers. While the age range is likely too small to reliably draw conclusions from, the lack of a dependence of F_{BSS} on cluster age could imply that whatever the preferred mechanism(s) of BSS formation, it occurs in globular clusters of every age with comparable frequencies. It should be noted that this result does not extend to open clusters. There is a clear correlation of blue straggler frequency with cluster age for open clusters between the ages of 10^8 and 10^{10} years (de Marchi et al., 2006). Cumulative BSS luminosity functions were analyzed for all 57 GCs. Unlike Piotto et al. (2004), we found no real difference between the BSLFs of the most massive clusters and those of the least massive clusters. In fact, we found no correlation between the shape of the cumulative luminosity function and any other cluster property. These results do not support the notion that differing interior chemical profiles cause collisionally-produced BSSs to have differing luminosities from those created via mass transfer or the coalescence of primordial binaries. It does, however, suggest that either the products of both formation mechanisms cannot be distinguished by their luminosity functions alone, or a single formation mechanism is operating predominantly in all environments.

Trends were also looked for in the brightest blue stragglers, since we suspected their enhanced brightnesses to imply a collisional origin. We also looked at the entire core blue straggler population in the most massive clusters (also thought to be predominantly a collisional population). No trends were observed. Therefore, even putatively collisional blue stragglers show no connection to their cluster environment.

What conclusions can we draw from this near-complete lack of connection between blue stragglers and their environment? We approached this project with the idea of looking only at blue stragglers formed through stellar collisions (those in the core, or the brightest blue stragglers in the core). Having found no correlations, we are forced to acknowledge that our prediction that core blue stragglers are predominantly formed through collisions may be incorrect. This is in disagreement with many arguments in the literature. Those arguments range from discussions of probable encounter rates (Hills & Day, 1976) to the detailed dynamical simulations of Mapelli et al. (2006). It should be noted that while collisions are not solely responsible for their production, they may still play an important role in BSS formation. Indeed, the fraction of close binaries has been found to be correlated with the rate of stellar encounters in GCs (Pooley et al., 2003). It is becoming increasingly clear that GCs represent complex stellar populations and that detailed models are required in order to accurately track their evolution.

It has also become clear, however, that blue stragglers are an elusive bunch. It appears more and more obvious that there are numerous factors working together to produce the populations that we observe. Even if we limit ourselves to consider only those blue stragglers created through binary mergers, we still need to include the effects of cluster dynamics since the binary populations of clusters will be modified through encounters (e.g. Ivanova et al., 2005). Contrary to what Davies et al. (2004) suggest, we do not feel we can reliably say that the effects of collisions will be to explicitly reduce the binary population in the core. Rather, it is likely that the distribution of periods, separations, and mass ratios will be modified through encounters but precisely

how remains difficult to predict. Indeed, dynamical processes act to reduce the periods in short-period binaries rather than destroy them, with the binaries at the lower end of the period distribution shifting to even shorter periods the fastest (Andronov et al., 2006). At the same time, wider binaries can be destroyed in clusters as a result of stellar interactions. Therefore, models of blue straggler populations need to be reasonably complex. In this thesis, we present observational constraints on those models. Blue straggler populations must be approximately constant for clusters of all ages, densities, concentrations, velocity dispersions, etc.; the number of blue stragglers decreases with increasing cluster mass; and the type, or luminosity function, of blue stragglers is apparently completely random from cluster to cluster. That the luminosity function data appears random perhaps should not have been a surprise. The current blue straggler luminosity function is a convolution of the blue straggler mass function and the blue straggler lifetimes.

There is one important cluster property for which we could not perform this analysis – the cluster binary fraction. If those clusters with a high binary fraction also have higher relative BSS frequencies then this might suggest a preferential tendency towards BSSs forming via coalescence. More importantly, such a trend could be indicative of less massive clusters having a higher frequency of binaries of the right type. That is, less massive clusters may be more likely to harbour binary systems with components in the right mass range and with the right separation to form blue stragglers in the lifetime of the cluster. It therefore seems wise to develop our knowledge of the types of binary systems commonly found in GCs, specifically the mass ratios, periods, and separations thereof. Preston & Sneden (2000) suggest that GCs either

destroy the primordial binaries that spawn long-period BS binaries like those observed in the Galactic field, or they were never home to them in the first place. This statement supports the notion that the majority of BSSs formed in globular clusters are the products of the mergers of close binaries, a claim that is not in disagreement with the results of this thesis. Work is required on both the observational and theoretical fronts in order to completely understand this ubiquitous, and frustrating, stellar population.

Bibliography

Andronov, N., Pinsonneault, M. H., & Terndrup, D. M. 2006, ApJ, 646, 1160

Davies, M. B., Piotto, G., & de Angeli, F. 2004, MNRAS, 349, 129

De Angeli, F., Piotto, G., Cassisi, S., Busso, G., Recio-Blanco, A., Salaris, M., Aparicio, A., & Rosenberg, A. 2005, AJ, 130, 116

de Marchi, F., de Angeli, F., Piotto, G., Carraro, G., & Davies, M. B. 2006, A&A, 459, 489

Djorgovski, S. & Meylan, G. 1994, AJ, 108, 1292

Ferraro, F. R., Paltrinieri, B., Fusi Pecci, F., Cacciari, C., Dorman, B., Rood, R. T., Buonanno, R., Corsi, C. E., Burgarella, D., & Laget, M. 1997, A&A, 324, 915

Ferraro, F. R., Sills, A., Rood, R. T., Paltrinieri, B., & Buonanno, R. 2003, ApJ, 588, 464

Harris, W. E. 1996, AJ, 112, 1487

Hills, J. G. & Day, C. A. 1976, Astrophys. Lett., 17, 87

Ivanova, N., Belczynski, K., Fregeau, J. M., & Rasio, F. A. 2005, MNRAS, 358, 572

Mapelli, M., Sigurdsson, S., Ferraro, F. R., Colpi, M., Possenti, A., & Lanzoni, B. 2006, MNRAS, 373, 361

Monkman, E., Sills, A., Howell, J., Guhathakurta, P., de Angeli, F., & Beccari, G. 2006, ApJ, 650, 195

Piotto, G., De Angeli, F., King, I. R., Djorgovski, S. G., Bono, G., Cassisi, S., Meylan, G., Recio-Blanco, A., Rich, R. M., & Davies, M. B. 2004, ApJ, 604, L109

Piotto, G., King, I. R., Djorgovski, S. G., Sosin, C., Zoccali, M., Saviane, I., De Angeli, F., Riello, M., Recio-Blanco, A., Rich, R. M., Meylan, G., & Renzini, A. 2002, A&A, 391, 945

Pooley, D. & Hut, P. 2006, ApJ, 646, L143

Pooley, D., Lewin, W. H. G., Anderson, S. F., Baumgardt, H., Filippenko, A. V., Gaensler, B. M., Homer, L., Hut, P., Kaspi, V. M., Makino, J., Margon, B., McMillan, S., Portegies Zwart, S., van der Klis, M., & Verbunt, F. 2003, ApJ, 591, L131

Press, W. H., Teukolsky, S. A., Vetterling, W. T., & Flannery, B. P. 1992, Numerical recipes in FORTRAN. The art of scientific computing (Cambridge: University Press, 2nd ed.)

Preston, G. W. & Sneden, C. 2000, AJ, 120, 1014

Pryor, C. & Meylan, G. 1993, in ASP Conf. Ser. 50: Structure and Dynamics of Globular Clusters, ed. S. G. Djorgovski & G. Meylan, 357

Sandquist, E. L. 2005, ApJ, 635, L73

Chapter 4

Dynamical Considerations

After analyzing the observations presented in Chapter 3 while searching for possible links between BSS formation and environment, we wanted to create a simple model in an effort to reproduce the general trends seen in the data. Globular clusters are home to extensive stellar populations whose members interact in a variety of ways over the course of their lives. As such, a thorough understanding of cluster dynamics and the subsequent evolution is required in order to make even the simplest of models. In particular, we must be able to track the various dynamical processes responsible for the creation, destruction, and migration of BSSs.

4.1 Globular Cluster Evolution

There are three primary mechanisms through which the exchange of stellar energies can progress in a cluster. The first is evaporation, in which stars having velocities exceeding the local escape speed are ejected from the cluster. As a result of stellar interactions, fluctuations in the gravitational field alter the velocities of the stars, both in magnitude and direction. Close encounters can

cause significant changes in velocity, whereas these changes tend to be much smaller in distant encounters. The net effect of these interactions continually results in stars being imparted with enough energy to escape the cluster potential. Clusters tend to reach sufficiently high densities for these effects to be significant during the collapse of the core (Gerhard, 2000).

The second mechanism describes the tendency of heavier stars to slow down and fall in towards the cluster center, a process that stems from the tendency of a cluster to evolve towards equipartition among stars of different mass. Because binary systems tend to be heavier than other members of a GC, the gravitational potential preferentially pulls them in towards the cluster center. The core typically evolves very quickly so that up to 50% of its total mass becomes tied up in binaries (Hut et al., 1992). Binary heating then acts to support the core against further collapse when binaries become more tightly bound post-encounter, adding to the translational kinetic energies of both single and binary stars. The total core mass can be maintained while dynamical processes destroy the binaries therein.

Finally, the third mechanism, referred to as the "gravothermal instability", is a process in which a confined system of gravitationally-interacting masses contracts upon releasing energy. In an isolated isothermal sphere having a sufficiently large density difference between the core and outer regions, the core can shrink in size, consequently heating up in the process and transferring its energy to the outer regions (Spitzer, 1987). Core-collapse becomes an especially important consideration in cluster evolution when it reaches a state of dynamical equilibrium that is, for all practical purposes, characteristic of

an isolated system. This "gravothermal instability" results in an increase in the central velocity dispersion that diffuses outwards, liberating heat from the core and fueling a runaway collapse (Spitzer, 1987).

Interactions between stars and binary or higher-order systems greatly affect cluster evolution. The collapse of the core can actually be postponed by interactions between stars. Specifically, primordial binaries are thought to be capable of postponing core contraction (Hut et al., 1992) by imparting translational kinetic energy to other nearby stars upon increasing their binding energy post-encounter. These encounters thus typically provide the cluster with a heat source. Even in the event of evaporation of these stars (or even binaries) from the cluster post-interaction, this mass-loss acts as an additional heat source since a reduction in the total mass of the cluster leads to a decrease in the total gravitational binding energy and a subsequent cluster expansion. A similar argument applies to mass loss from individual stars when gas is ejected as a result of processes like stellar winds.

Many aspects of the evolution of GCs past core-collapse remain uncertain, though the average behavior has been firmly established. For instance, the half-mass radius of an isolated GC expands as:

$$R_h(t) \propto t^{2/3}, \tag{4.1}$$

where t is the time since core bounce (McMillan et al., 1990). Similarly, the velocity dispersion has been found to decrease according to:

$$\sigma(t) \propto t^{-1/3} \tag{4.2}$$

These relations can be derived from first principles by relating the virial theorem to the rate of mass loss due to stellar evaporation without any a priori knowledge of the mode of energy generation in the core (McMillan et al., 1990). The rate of cluster expansion does, however, vary with the primary source of energy generation in the core, whether it be binary-hardening, distant encounters, exchange interactions, etc. (Ostriker, 1985).

Most of the clusters in Piotto et al.'s (2002) database are not post core-collapse. It thus seems reasonable in these cases to assume that (1) the gravitational potential energy of the cluster, its velocity distribution function, as well as all other cluster properties are independent of time since these clusters are still undergoing core-collapse and are hence not as dynamically evolved and (2) that the cluster has complete spherical symmetry.

Post-core collapse clusters are thought to be primarily, if not entirely, home to dynamically-formed binaries since their primordial counterparts will have either been disrupted, destroyed, or ejected by this point in the cluster evolution (Lightman & Fall, 1978). As such, different assumptions should be applied to post-core collapse clusters as opposed to other, less-evolved stellar systems. In particular, the binary fraction should change in dynamically evolving clusters while in post-core collapse systems it should remain more or less constant.

4.2 Rate of Migration into and out of the Core

In the data presented in Chapter 3, we focused only on those stars found within one core radius of the cluster center in an effort to isolate as best as

we could a single, dynamically-uniform cluster environment. Consequently, in setting out to model the observations, we must pay particular attention to the dynamical processes responsible for stellar (especially BSS) migration into and out of the core. The following discussion concentrates on the mechanism by which mass segregation mediates the radial distribution of stellar masses in a cluster.

For a simple and very rough overall picture of cluster evolution, consider the collapse of a cluster composed of stars of a single mass. As outlined above, this collapse is thought to progress in two phases: an evaporative phase followed by a runaway collapse of the core (Cohn, 1980). Most of the evolution is dominated by the evaporative phase, during which time the core shrinks and gets denser as stellar collisions act to eject stars from the central cluster potential. Eventually, the evolution speeds up as the cluster becomes gravothermally unstable and the core contracts further still, albeit more rapidly (Gerhard, 2000).

Real clusters, however, comprise stars having a range of masses. Observations suggest that present-day GCs are populated by stars having a relatively narrow mass range of around 0.1 $M_{\odot}$ at the faint end of the main-sequence (e.g. de Marchi & Paresce, 1997) up to 1-2 $M_{\odot}$ for objects like primordial binaries and blue stragglers (e.g. Bailyn, 1995). This lower mass cut-off stems from the fact that the equipartition of energy should result in an average velocity for these lighter stars that is sufficiently large for them to escape the cluster potential (Spitzer, 1969). A similar process occurs in the core as well and the lighter stars are accelerated through encounters with stars having different

masses. Consequently, lighter stars are ejected from the core at a higher rate than are heavier stars (Spitzer & Harm, 1958). Even though a greater fraction of these light stars are lost from the cluster than are background stars, many are retained in the halo and can even increase their number density in the outer regions (Fregeau et al., 2002).

GC ages tend to exceed their central relaxation times by a factor lying somewhere in the range 10-10^3 (Fregeau et al., 2002). Consequently any mass segregation occurring in and around the cores of GCs must be due to dynamical evolution. Massive MS stars, binaries, primordial black holes (around 10 $M_\odot$), and other stellar bodies more massive than a few times $M_\odot$ populated GCs earlier in their dynamical evolution than did their less-massive counterparts (Fregeau et al., 2002). In younger stellar groupings, however, it is thought that the present-day mass segregation occurring may still be indicative of the initial cluster conditions (Portegies Zwart et al., 2002).

Numerical models of clusters that are comprised of stars of different masses have all shown rapid mass stratification, with the heaviest stars tending to migrate into the core within one to two t_h's (Spitzer & Shull, 1975). As the more massive stars impart kinetic energy to their nearby lighter counterparts, they tend towards lower random velocities and so the cluster gravitational potential draws them inwards towards the center. This process is easily masked by the effects of an already contracting core and in fact acts to shorten the timescale required for a cluster to evolve from birth to core collapse (Spitzer, 1987). It is impossible for clusters to experience both dynamical and thermal equilibrium simultaneously, however (Spitzer, 1969). The former is defined by

the scalar virial theorem, where $< T >$ and $< W >$ are, respectively, the total kinetic and potential energies of the system:

$$2 < T > + < W >= 0 \tag{4.3}$$

and the latter is defined by equipartition of energy among components of different mass m_i (Meylan, 2000):

$$m_i < v_i^2 >= 3kT \tag{4.4}$$

Every species i in Equation 4.4 must have the same temperature T so there is an exchange of energy between them. However, in the event that every star has the same temperature, the most massive stars will be slower and mass segregation will act to prevent the system from reaching a state of dynamical equilibrium as these heavier stars drift inwards towards the cluster center.

If equipartition cannot be reached, the more massive stars continue their inward drift until they start to dominate the cluster's gravitational potential in the core. The heavier stars will then undergo a gravothermal collapse to form a small, dense core populated predominantly by the most massive stars. The potential for a two-component cluster to attain thermal equilibrium can be approximated using the "Spitzer stability condition" (Spitzer, 1969):

$$S = (M_2/M_1)(m_2/m_1)^{3/2} \lesssim 0.16, \tag{4.5}$$

where M_1 and M_2 represent the total masses of species 1 and 2, respectively. If S is found to be less than 0.16 or so, the cluster is "Spitzer stable" and the two mass-components will eventually attain thermal equilibrium. On the other hand, if S surpasses 0.16, the system is "Spitzer unstable" and equipartition

cannot be reached. In order for equipartition of energy to be satisfied in a star cluster, it must be populated by stars of equal temperature. In equipartition, $m_2 < v_2^2 >= m_1 < v_1^2 >= 3m_1\sigma^2$, where σ is the 1-D velocity dispersion of the lighter stars (Meylan, 2000). If a cluster is "Spitzer unstable", the range of stellar masses is too large and the distribution too extreme for every star within the cluster to have the same temperature. Clusters having more or less equal mass components are therefore the most likely to reach a state of thermal equilibrium.

The timescale for a group of massive stars of mass m_2 to lose energy to lighter stars of mass m_1, called the equipartition time, can be approximated as (Spitzer, 1969):

$$t_{eq} = \frac{(< v_1^2 > + < v_2^2 >)^{3/2}}{8(6\pi)^{1/2}\rho_{01}G^2 m_2 \ln N_1}, \tag{4.6}$$

where we set the stellar density equal to its value at the center of the system. If we assume equal temperatures such that $< m_1 v_1^2 >=< m_2 v_2^2 >$, we get (Gerhard, 2000):

$$t_{eq} = 1.2\frac{m_1}{m_2} t_{rc}(m_1), \tag{4.7}$$

where t_{rc} is the central relaxation time. The important point to draw from Equation 4.7 is that the time required for cluster relaxation to begin playing a significant dynamical role exceeds that for mass segregation of the most massive stars (Gerhard, 2000).

Crude estimates based on semi-analytic methods have put the equipartition time somewhere between 10^7 and 10^8 years (Spitzer, 1969). Numerical N-body simulations of two-component globular clusters have been performed in which most objects are assumed to have some mass m_1 while the objects of mass

m_2 are said to form a 'tracer population' such that the total component mass ratio is much less than unity (e.g. Fregeau et al., 2002). Light tracers, for which $\mu = m_2/m_1 < 0.1 - 0.4$, were found to be ejected from the cluster core within one central relaxation time, or somewhere in the range 10^7-10^8 years for most GCs. Consequently, stars less massive than around 0.25 $M_\odot$ should be nearly entirely absent in their cores (Fregeau et al., 2002). Clusters with heavy tracers for which $\mu = m_2/m_1 > 1$, on the other hand, have mass segregation timescales, τ_0, that vary as $1/\mu$. In particular, for a wide range of initial concentrations and mass ratios, it was found that $\tau_0/t_r = C/\mu$, where C is a constant that ranges from about 0.5 - 1 (Fregeau et al., 2002).

For decades, the characteristically high stellar densities in GCs prevented clear observational evidence of mass segregation from being uncovered. In recent years, however, differences in the radial distributions of stars of different mass have been definitively observed with the Hubble Space Telescope. In particular, evidence comes from the slope of the mass function (which is continuous) decreasing at smaller and smaller radii in GCs, as has been approximated from observed luminosity functions at various distances from the cluster center or even from colour gradients (Howell et al., 2001). One of the most detailed such studies was done by Anderson (1997) who used HST/FOC and HST/WFPC2 data to show that mass segregation is occurring in the cores of three galactic globular clusters, namely M92, 47 Tuc, and Omega Centauri. After constructing luminosity functions for each cluster at two different spots in the core, Anderson (1997) compared them to those from King-Mitchie multi-mass models and was able to rule out completely any model without mass segregation. M92 displayed results very similar to those for 47 Tuc, an out-

come not altogether unexpected due to the fact that both clusters share similar structural parameters and hence similar central relaxation times of around 100 Myr. Omega Cen, on the other hand, is an especially massive GC with a core relaxation time of $t_c = 6$ Gyr and so has had little time to relax dynamically. As anticipated, the model LFs computed at its center exhibited very little mass segregation (Anderson, 1997).

The term "mass segregation" therefore encompasses a host of complex dynamical processes that remain poorly understood theoretically, including mass stratification, energy equipartition, gravothermal contraction and at times even gravothermal instabilities (Heggie et al., 1998). These processes act together to push clusters towards a state of dynamical equilibrium - less massive stars gain kinetic energy and move to larger radii while more massive stars lose kinetic energy and sink to the cluster center. It is the net result of these effects that we are concerned with here since we are interested in evaluating the rate of migration of blue straggler stars - or likely progenitors - into the cluster core. It should therefore be reiterated that binary systems become much more centrally concentrated than do single stars as a direct consequence of mass segregation (Hut et al., 1992), though these also tend to be destroyed via dynamical processes as the cluster ages. Indeed, binary segregation is particularly important in fueling the initial collapse of cluster cores.

4.3 Relaxation Timescales and the Rate of Stellar Evaporation

In designing our model, we set out to be able to predict the number of BSSs in the cores of GCs. In so doing, we needed a quantitative means of describing the evolution or rate of dynamical relaxation. We also needed an estimate for the rate of escape of stars from the cluster potential and wanted to know how this could in turn affect the subsequent evolution in the core. As such, a discussion of relaxation timescales and stellar evaporation in GCs follows.

The "relaxation time", t_r, refers to the time required for deviations from a Maxwellian velocity distribution to be noticeably decreased.

For simplicity, the relaxation time can be expressed in terms of only the total number of stars N, the stellar mass m, and the stellar radius R (Lightman & Fall, 1978):

$$t_r \cong 7 \times 10^8 (\frac{N}{10^5})^{1/2} (\frac{m}{M_\odot})^{-1/2} (\frac{R}{5pc})^{3/2} \text{ years} \tag{4.8}$$

As first demonstrated by Antonov (1962), in the initial stages of cluster evolution the evaporation of stars progresses due to the Galaxy's gravitational influence, which in turn causes the central regions to begin to contract. When the central density gets high enough, a gravothermal instability kicks in (locally) and the core starts to shrink progressively faster. The timescale for core relaxation, t_c, can be written (Lightman & Shapiro, 1977):

$$t_c = 1.55 \times 10^7 \frac{(M_\odot/m)}{\log(0.5 M_t/m)} (\frac{\sigma}{kms^{-1}}) (\frac{r_c}{pc})^2 \text{ years}, \tag{4.9}$$

where m is the mean stellar mass in the core and M_t is the total cluster mass. This quantity can then be used to find a more convenient expression for the relaxation time (Davies, 1995):

$$t_r = t_c(r/r_c)^2 \tag{4.10}$$

The relaxation time in the cluster center often deviates significantly from that in the outer regions of the cluster, making the half-mass relaxation time, t_h, a particularly useful timescale. The half-mass relaxation time is defined as the value of t_r obtained by making the stellar number density n equal to the average particle density within r_h (the radius enclosing half the cluster mass where $r_h = GM^2/(2|E|)$) as well as by setting v_m^2 equal to the mean square velocity for the whole cluster as obtained from the virial theorem.

$$t_h = 1.7 \times 10^5 \frac{(r_h(pc))^{3/2} N^{1/2}}{(m/M_\odot)^{1/2}} \text{ years} \tag{4.11}$$

The half-mass relaxation time, as given by Equation 4.11, changes relatively little during the evolution of some clusters due to the competing effects of expansion in the cluster outskirts and contraction in the central regions, which can keep r_h more or less constant as the cluster evolves. The central relaxation time, on the other hand, goes down significantly over the course of cluster evolution as a result of the central density increasing faster than v_m^3 at $r = 0$ (Spitzer, 1987). Central relaxation times have been calculated to be around 10^7-10^9 years in GCs (Gerhard, 2000), while half-mass relaxation times are expected to be larger and lie in the range 10^8-10^{10} years (Davies, 1995). The core relaxation time is thought to occur on a timescale that is at most a few times larger than t_h (Davies, 1995).

The timescale for core-collapse (from start to finish), $t_{collapse}$, is thought to be proportional to the half-mass relaxation time and the central relaxation time. Specifically, $t_{collapse}/t_h = 16$ or $t_{collapse}/t_c = 60$ (Cohn, 1980). It should be noted, however, that $t_{collapse}/t_h$ will be less than 16 for especially centrally-concentrated clusters (Grabhorn et al., 1993).

The rate of escape of stars from a cluster can be divided into two subcategories. The first and rarer of the two, ejection, involves a single close encounter between stars that results in one of them acquiring enough energy to surpass the local escape speed, v_{esc}, and depart from the cluster. This process has a timescale of (Hénon, 1961):

$$t_{ej} \simeq 1.1 \times 10^3 t_h \ln 0.4N \sim 10^4 t_h \tag{4.12}$$

The second escape mechanism, evaporation, has a more dramatic impact on the rate of escape of stars from the cluster potential than does ejection. In this case, stars interact with each other via repeated weak encounters and experience a gradual build-up of energy until $v \geq v_{esc}$, at which point they escape from the cluster. Detailed calculations have shown that (Spitzer & Thuan, 1972):

$$t_{ev} \equiv -\frac{N}{dN/dt} \simeq 300 t_h \tag{4.13}$$

The important point here is that the resultant velocities of the escaping stars only slightly exceed v_{esc}. The total energy of the cluster thus stays more or less fixed, but is distributed among fewer stars. Consequently, as the density increases in the core, the evaporation process speeds up and the cluster continues shrinking towards a state of negligible mass and radius. The least massive stars are expected to escape the fastest while the heaviest stars sink towards

the central regions of the cluster due to mass segregation (Lee & Goodman, 1995). The timescale for evaporation can also be related to the cluster relaxation time (using Equation 4.8 for t_r) (Allen & Bastien, 1996):

$$t_{ev} \cong 136 t_r \tag{4.14}$$

A steady tidal force coming from a fixed direction can noticeably impact the rate of evaporation of stars from the cluster potential by decreasing the required escape energy. Real clusters generally experience tidal forces from the Galaxy which cause stars to evaporate more readily if their separation from the cluster center is greater than the tidal cut-off distance, r_t, given by (Spitzer, 1987):

$$r_t^3 = \frac{M_t}{2M_G} R_G^3, \tag{4.15}$$

where M_t is again the total cluster mass, M_G is the mass of the Galaxy, and R_G is the distance separating the Galaxy from the cluster center. The relative reduction in escape energy, denoted by γ, can be found by evaluating the ratio of the tidally-limited cluster potential to that of isolated clusters (Spitzer, 1987):

$$\gamma = \frac{5 r_h}{4 r_t} \tag{4.16}$$

The ratio r_h/r_t can vary significantly between clusters though models of such tidally-limited systems suggest a typical value of 0.145 (Hénon, 1961). This then gives $\gamma = 0.18$ and leads to an escape probability per t_h of $\epsilon_e = 2.0 \times 10^{-2}$. Note that this rough estimate of ϵ_e for the tidally-limited case is roughly a factor of three higher than that found in the isolated case. While this is a rough estimate, it supports the notion that stars escape from the cluster potential

with a significantly greater frequency in the tidally-limited scenario. Indeed, detailed numerical solutions performed by Hénon (1961) give $\epsilon_e = 4.5 \times 10^{-2}$ for this escape probability.

For modeling purposes, the assumption of spherical symmetry for clusters makes evaluating the net effects of various dynamical processes a great deal simpler. However, the gravitational influence of the Galaxy clearly plays an important role in the rate of stellar evaporation and tends to increase it by about a factor of three. This rough factor thus needs to be accounted for in GC models in order to properly estimate the rate of escape of stars from a spherically-symmetric cluster.

4.4 Contribution from Collisions

Globular clusters are home to sufficiently high number densities (up to 10^5 stars pc^{-3}) that the timescales for encounters between stars can be comparable to the ages of the oldest GCs (Davies, 1996). That is, a great many of the stars populating GCs will have undergone at least one collision or close encounter by the end of their lives (Laycock & Sills, 2005). The timescale for stellar encounters between two single stars to operate within a cluster can be approximated as (Davies, 1996):

$$\tau_{coll} = \frac{1}{n\sigma v}, \tag{4.17}$$

where σ is the cross-section for two stars having a relative velocity at infinity of $v_{\rm inf}$ to pass within a distance R_{min} after gravitational focussing occurs and is given by (Davies, 1996):

$$\sigma = \pi R_{min}^2 (1 + \frac{v^2}{v_{\rm inf}^2}) \tag{4.18}$$

The number density of single stars of mass m is denoted by n, while v represents the relative velocity of the two stars at closest approach during an encounter such that $v^2 = 2G(m_1 + m_2)/R_{min}$. The second term in Equation 4.18 is a consequence of the gravitational force of attraction between the stellar pair under consideration. Two extreme regimes for the timescale between single-single collisions can be considered separately (Davies, 1996):

$$\tau_{coll1+1} = 7 \times 10^{10} (\frac{10^5 pc^{-3}}{n})(\frac{v_{\rm inf}}{10 km/s})(\frac{R_\odot}{R_{min}})(\frac{M_\odot}{M}) \text{ years for } v \gg v_{\rm inf}, \tag{4.19}$$

and

$$\tau_{coll1+1} = 7 \times 10^{12} (\frac{10^5 pc^{-3}}{n})(\frac{100 km/s}{v_{\rm inf}})(\frac{R_\odot}{R_{min}})^2 \text{ years for } v \ll v_{\rm inf} \tag{4.20}$$

Note that the regime $v \ll v_{\rm inf}$ typically applies to regions having exceptionally high velocity dispersions, as tends to be the case in galactic nuclei. On the other hand, the regime $v \gg v_{\rm inf}$ is more suitable for systems having low velocity dispersions, as is the case in globular clusters. Thus, for single star collisions in GCs, $\tau_{coll} \propto 1/R_{min}$ (Davies, 1996).

In terms of the core radius r_c, the central number density n_0, the root-mean-square velocity V_{rms}, the individual stellar mass m_* and the stellar radius R_*, the mean timescale between single-single collisions in the cores of GCs is (Leonard, 1989):

$$\tau_{coll1+1} = 1.1 \times 10^9 (\frac{1pc}{r_c})^3 (\frac{10^3 pc^{-3}}{n_0})^2 (\frac{V_{rms}}{5 km/s})(\frac{0.5 M_\odot}{m_*})(\frac{0.5 R_\odot}{R_*}) \text{ years} \tag{4.21}$$

A similar expression can be found for the timescale needed for single-binary encounters to operate within a cluster. For a binary of separation d, this timescale is (Davies, 1995):

$$\tau_{coll1+2} = 3 \times 10^{11} \frac{1}{n_4} (\frac{d}{R_\odot})^{-1} \text{ years}, \tag{4.22}$$

where n_4 is the total number density of stars in units of 10^4 pc^{-3}.

Finally, the timescale between binary-binary collisions in a globular cluster can be estimated as (Leonard, 1989):

$$\tau_{coll2+2} = 1.7 \times 10^7 (\frac{1pc}{r_c})^3 (\frac{10^3 pc^{-3}}{n_0})^2 (\frac{V_{rms}}{5km/s}) (\frac{0.5M_\odot}{m_*}) (\frac{1AU}{a}) \text{ years}, \tag{4.23}$$

where a is the semi-major axis of the binary system. Note that Leonard (1989) have assumed that the binary frequency is 100% in the core and that collisions in the outskirts can be ignored. While a binary fraction of 100% is expected to be uncharacteristic of real clusters, Equation 4.23 provides a good first approximation and will be adjusted in Chapter 5 to be more appicable to cluster cores.

For a close encounter between single stars to be dynamically significant it is generally thought that $R_{min} \leq 3\text{R}_\odot$ is required (Davies et al., 1992). For a close encounter between a single star and a binary pair to be dynamically significant, however, we require $R_{min} \simeq a$, where a represents the semi-major axis of the binary system. Even in the case of a binary with a semi-major axis on the order of 1 AU ($\equiv$ 216 R$_\odot$), $\tau_{coll} \ll 10^{10}$ years and so such interactions will typically be important even in GCs with low binary fractions (Davies, 1996). Encounters between two binary systems also require $R_{min} \simeq a$ to be significant. The binary fraction therefore needs to be quite high ($\geq$ 30%)

in order for the importance of binary-binary interactions to surpass that of binary-single interactions in GCs.

Numerous studies suggest that quick core collapse fuels collisional processes and sparks the growth of a very massive star (VMS) in the centers of most GCs via repeated mergers. Most of the mass that comprises the VMS comes from the upper-most portion of the IMF ($M_* \simeq 100$ $M_\odot$) as a result of strong mass segregation (Freitag et al., 2004). Because the expected time between mergers is thought to be less than the thermal timescale of the VMS, its structure is likely considerably more diffuse than that of a MS star and displays typical accretion rates that exceed 10^{-3} $M_\odot yr^{-1}$ (Freitag et al., 2004). Whether or not the VMS will eventually give rise to an intermediate-mass BH remains unknown since strong stellar winds can act to reduce the VMS mass (unless the metallicity is very low) once its collisional growth has slowed.

It is clear that environment, and in particular the binary fraction, has an appreciable impact on the nature of the dominant stellar interactions occurring within a GC. It is unfortunate that this parameter is so poorly understood and attempting to at least constrain it in GCs could prove a crucial step towards isolating the dominant mode of BSS formation as well as the rate at which it operates.

4.5 Contribution from Binaries

Apart from collisions, the only other currently favored BSS formation mechanism is binary coalescence. Though a great deal of work still needs to be done on both observational and theoretical fronts, we present some of the more im-

portant considerations that must be addressed in attempting to model the effects of such interactions.

Consider an evolving binary system whose stars are point masses that are undergoing mass-transfer in a circular orbit. Then, if the orbital decay is fueled by systemic angular momentum losses $\dot{J}_{sys}$ like gravitational radiation and magnetic braking, the separation between components changes according to the relation (D'Souza et al., 2006):

$$\frac{\dot{a}}{2a} = (\frac{\dot{J}}{J_{orb}})_{sys} - \frac{\dot{M}_d}{M_d}(1-q), \tag{4.24}$$

where $q = M_d/M_a$, M_d is the donor's mass, M_a is the accretor's mass, and the total, solely orbital, angular momentum is (D'Souza et al., 2006):

$$J_{tot} = J_{orb} = \frac{M_d M_a}{M_a + M_d} a^2 \Omega = M_d M_a (\frac{Ga}{M_a + M_d})^{1/2} \tag{4.25}$$

Note as well that the dots indicate derivatives with respect to time and $\dot{M}_a = -\dot{M}_d$ is assumed so that mass is conserved. Moreover, the binary's orbital frequency Ω, which can be used to find the orbital period via the relation $P = 2\pi/\Omega$, is given by:

$$\Omega = (\frac{G(M_a + M_d)}{a^3})^{1/2} \tag{4.26}$$

If we take the finite size of the stars into account, then Equation 4.24 no longer accurately describes the orbital evolution and two new terms need to be introduced (Marsh et al., 2004):

$$\frac{\dot{a}}{2a} = (\frac{\dot{J}}{J_{orb}})_{sys} - (\frac{\dot{J}_a + \dot{J}_d}{J_{orb}})_{tides} - \frac{\dot{M}_d}{M_d}(1 - q - \sqrt{(1+q)r_h}), \tag{4.27}$$

where J_a and J_d are the spin angular momenta of the accretor and donor stars, respectively, and $r_h \equiv R_{circ}/a/$ is the circularization radius. The second

term on the right-hand-side of Equation 4.27 accounts for changes in the spin angular momenta caused by tidal forces, whereas the term containing r_h relates to the specific angular momentum carried by the stream and accounts for the rate of its transfer to the accretor.

In order to approximate the overall rate of binary coalescence in a cluster and evaluate the number of suitable mergers as a function of time one needs to take into account: (1) the binary fraction; (2) the initial mass function and the distribution of masses in binary systems; (3) the distribution of orbital periods and separations; (4) the distribution of orbital eccentricities; and (5) the initial spatial distribution of binaries in the cluster. We will focus primarily on the first three considerations since simple approximations can be carried out to account for the range of possible orbital eccentricities, and mass segregation is expected to cause most binaries to migrate in towards the cluster center relatively early on in a cluster's lifetime.

Binaries with wide separations having periods on the order of years have larger collisional cross sections and so typically experience more encounters with other single and binary stars. BSSs in the cores of GCs are therefore, for the most part, probably not a product of mass-transfer from an evolved donor in binaries with wide separations since these systems tend to be disrupted before this can happen (Heggie, 1975). Wide binaries will likely only survive in the cluster's outer regions due to their high collisional cross-sections and the increased rate of encounters in the core. Short-period binaries, on the other hand, greatly affect the dynamical evolution of a cluster (Heggie, 1975) and, in fact, their mergers could be the dominant formation scenario for BSSs

in GCs. Dynamical processes act to reduce the periods in these systems, with the binaries at the lower end of the period distribution shifting to even shorter periods the fastest (Andronov et al., 2006). In so doing, close binaries become more tightly bound by transferring energy to nearby single stars or other wide binaries that they undergo close encounters with. Tight primordial binaries (PBs) should thus merge early on in the lifetime of a cluster. Since the average BSS lifetime, t_{BSS}, is on the order of 1-2 Gyr (Lombardi et al., 2002), PB mergers should terminate the MS life of the stars and, due to their old ages, they should consequently be absent in most GCs (Lombardi et al., 2002). The interplay between wide and close binary systems may help to explain the peculiar radial distribution of BSSs observed in clusters like 47 Tuc (Mapelli et al., 2004).

For a complete picture, one needs to also consider the rate of binary formation occurring both in the core and in the outskirts. Dynamical effects are not thought to play as important a role in the outer regions of a cluster and so it is thought that both binary formation and destruction can be neglected there. Indeed, the majority of binary destruction takes place within a few core radii of the cluster center since mass segregation acts to migrate these systems into the core. Moreover, any binaries formed in the core will have short-periods and so will merge rapidly (Heggie, 1975).

The formation of binary systems is thought to occur in the cores of GCs with enough frequency to be dynamically significant. Numerical N-body simulations suggest, however, that this process has a greater impact on the dynamical evolution therein than on the direct formation of BSSs via the merger

scenario (Hut et al., 1992). The energy released by the formation of a single binary pair can be comparable to the kinetic energy of the entire system and can act to greatly slow the rate of core collapse. Even for N-values comparable to what is expected in a real GC ($N = 10^5 - 10^6$), typically only a few binaries will exist in the core at a given time as a result of the system trying to balance energy-loss in the outer regions with the energy created by the binaries.

Heggie (1975) showed that hard binaries in the presence of a Maxwellian distribution of field particles harden at a fixed rate. The constancy of this rate implies that once all primordial binaries have either been ejected or disrupted, there will exist a constant number of binaries in the core. The total number of binaries in an evolved core (post-core collapse) can thus be approximated as (Goodman, 1984):

$$N_b = 11\frac{G^3 m_*^3 n_c}{\sigma_c^8}|\Phi_c|N_c, \tag{4.28}$$

where m_* is the particle mass, n_c is the number density of particles, σ_c is the 1-D central velocity dispersion, Φ_c is the central potential depth, and N_c is the total number of particles in the core as given by $N_c = M/m_*$. It follows from Equation 4.28 that $N_b \propto N^{-1/3}$ and so those clusters having the most stars will consequently have the fewest binaries.

The formation of binaries is particularly important during the process of core collapse. Encounters with single stars and with other binaries affect the cluster contraction and ultimately influence the rate of collapse as well as the resulting core radius (Spitzer, 1987). In order to predict the number of binaries in cores that have not undergone core collapse, the number of primordial binaries must be taken into account as well as their rates of ejection, disruption

and destruction. Binaries can form in significant numbers via tidal capture events in which two stars pass within a few stellar radii and become gravitationally bound. Three-body interactions can also result in the formation of binary systems, albeit only at very high densities. In this case, one of three stars gains additional energy, leaving the other two bound in a tight binary system. The timescale for this process is (Binney & Tremaine, 1987):

$$t_3 = N_c^2 \ln N_c t_{r0}, \tag{4.29}$$

where N_c is the total number of stars in the core. This suggests that with each central relaxation time that passes, $1/N_c \ln N_c$ three-body binaries form. That is, if the final collapse of the core ends up being fueled by more than 100 of the most massive stars, the formation of three-body binaries becomes completely negligible (Gerhard, 2000).

In the next chapter, we will use all of the above considerations to create a model to predict the number of blue stragglers in the cores of GCs.

Bibliography

Allen, E. J. & Bastien, P. 1996, ApJ, 467, 265

Anderson, A. J. 1997, Ph.D. Thesis

Andronov, N., Pinsonneault, M. H., & Terndrup, D. M. 2006, ApJ, 646, 1160

Antonov, V. A. 1962, Solution of the problem of stability of stellar system Emden's density law and the spherical distribution of velocities (Vestnik Leningradskogo Universiteta, Leningrad: University)

Bailyn, C. D. 1995, ARA&A, 33, 133

Binney, J. & Tremaine, S. 1987, Galactic dynamics (Princeton, NJ, Princeton University Press)

Cohn, H. 1980, ApJ, 242, 765

Davies, M. B. 1995, MNRAS, 276, 887

Davies, M. B. 1996, in IAU Symp. 174: Dynamical Evolution of Star Clusters: Confrontation of Theory and Observations, ed. P. Hut & J. Makino, 243

Davies, M. B., Benz, W., & Hills, J. G. 1992, ApJ, 401, 246

de Marchi, G. & Paresce, F. 1997, ApJ, 476, L19

D'Souza, M. C. R., Motl, P. M., Tohline, J. E., & Frank, J. 2006, ApJ, 643, 381

Fregeau, J. M., Joshi, K. J., Portegies Zwart, S. F., & Rasio, F. A. 2002, ApJ, 570, 171

Freitag, M., Atakan Gürkan, M., & Rasio, F. A. 2004, ArXiv Astrophysics e-prints, astro-ph/0410327

Gerhard, O. 2000, in ASP Conf. Ser. 211: Massive Stellar Clusters, ed. A. Lançon & C. M. Boily, 12

Goodman, J. 1984, ApJ, 280, 298

Grabhorn, R. P., Irwin, J. A., Cohn, H. N., & Lugger, P. M. 1993, in ASP Conf. Ser. 50: Structure and Dynamics of Globular Clusters, ed. S. G. Djorgovski & G. Meylan, 131

Heggie, D. C. 1975, MNRAS, 173, 729

Heggie, D. C., Giersz, M., Spurzem, R., & Takahashi, K. 1998, Highlights of Astronomy, 11, 591

Hénon, M. 1961, Annales d'Astrophysique, 24, 369

Howell, J. H., Warren, J. A., Guhathakurta, P., Gilliland, R. L., Albrow, M. D., Sarajedini, A., Brown, T. M., Charbonneau, D., Burrows, A. S., Cochran, W. D., Baliber, N., Edmonds, P. D., Frandsen, S., Bruntt, H., Lin, D. N. C., Vogt, S. S., Choi, P., Marcy, G. W., Mayor, M., Naef, D., Milone, E. F., Stagg, C. R., Williams, M. D., Sigurdsson, S., & VandenBerg, D. A. 2001, in Bulletin of the American Astronomical Society, 1182

Hut, P., McMillan, S., Goodman, J., Mateo, M., Phinney, E. S., Pryor, C., Richer, H. B., Verbunt, F., & Weinberg, M. 1992, PASP, 104, 981

Laycock, D. & Sills, A. 2005, ApJ, 627, 277

Lee, H. M. & Goodman, J. 1995, ApJ, 443, 109

Leonard, P. J. T. 1989, AJ, 98, 217

Lightman, A. P. & Fall, S. M. 1978, ApJ, 221, 567

Lightman, A. P. & Shapiro, S. L. 1977, ApJ, 211, 244

Lombardi, Jr., J. C., Warren, J. S., Rasio, F. A., Sills, A., & Warren, A. R. 2002, ApJ, 568, 939

Mapelli, M., Sigurdsson, S., Colpi, M., Ferraro, F. R., Possenti, A., Rood, R. T., Sills, A., & Beccari, G. 2004, ApJ, 605, L29

Marsh, T. R., Nelemans, G., & Steeghs, D. 2004, MNRAS, 350, 113

McMillan, S., Hut, P., & Makino, J. 1990, ApJ, 362, 522

Meylan, G. 2000, in ASP Conf. Ser. 211: Massive Stellar Clusters, ed. A. Lançon & C. M. Boily, 215

Ostriker, J. P. 1985, in IAU Symp. 113: Dynamics of Star Clusters, ed. J. Goodman & P. Hut, 347–357

Portegies Zwart, S. F., Makino, J., McMillan, S. L. W., & Hut, P. 2002, ApJ, 565, 265

Spitzer, L. 1987, Dynamical evolution of globular clusters (Princeton, NJ, Princeton University Press)

Spitzer, Jr., L. & Shull, J. M. 1975, ApJ, 201, 773

Spitzer, L. J. 1969, ApJ, 158, L139

Spitzer, L. J. & Harm, R. 1958, ApJ, 127, 544

Spitzer, L. J. & Thuan, T. X. 1972, ApJ, 175, 31

Chapter 5

Modeling the Data

5.1 Predicting the Number of BSSs in the Core

After considering the various dynamical processes operating in GCs, we must decide which ones will have the greatest impact on F_{BSS} as well as how exactly it will be affected. We must also integrate our current observational knowledge of BSS populations into this overall picture of cluster evolution. Consequently, in order to predict the number of BSSs produced in a cluster as a function of time there are a few additional considerations that must be taken into account. First, BSSs seem to adhere to a bimodal spatial distribution, with a peak in the cluster core, a subsequent drop-off at intermediate radii and then another peak at larger radii (Ferraro et al., 2004). As such, there appears to exist a "zone of avoidance" in which BSSs do not form with any appreciable frequency. Indeed, it is possible that the BSSs we do see in the "zone of avoidance" are in the process of migrating inwards to the cluster center or are being ejected from the core. In order to approximate the number

of BSSs in the core at a given cluster age, we must take into account both the rate of formation within the core as well as the rate of BSS migration into and out of the core.

Clearly, different considerations and assumptions should be implemented in the core versus the outskirts. It has been proposed that the "zone of avoidance" is primarily the result of two separate formation mechanisms occurring in the inner and outer regions of the cluster, with mass transfer in primordial binaries dominating in the latter and merger-inducing stellar encounters dominating in the former (Ferraro et al., 1997; Mapelli et al., 2006). Indeed, as a direct consequence of the differing physical processes involved and the various rates at which they occur, it has been proposed that these two formation scenarios could produce strikingly different, observationally-distinguishable luminosity functions (Bailyn & Pinsonneault, 1995). One difficulty associated with this hypothesis, however, is that primordial binaries are expected to settle to the cluster center relatively quickly since relaxation times are usually less than 1 Gyr (Djorgovski, 1993). The question of whether or not there will be enough PBs left in the outskirts of the cluster to account for the rise in relative BSS frequencies in GCs at these larger radii is therefore an important one. Simulations suggest, however, that the majority of the PBs born at large radii ($\sim 60r_c$) with semi-major axis $a \geq 30r_c$ still have a comparable semi-major axis after 12 Gyr (Mapelli et al., 2004).

Alternatively, Sigurdsson et al. (1994) suggested that the external population of BSSs were created in the core and then got kicked out to the outer regions as a result of the recoil from stellar interactions. Binaries that get

ejected from the core are quick to drift back inwards due to mass segregation, stimulating an overall central concentration of BSSs. A greater recoil in the more energetic interactions will cause the stars to be ejected to larger distances and will take longer to fall back in. These high energy kicks could help account for the overabundance of BSSs seen at larger radii. It seems unlikely, however, that the BSSs in a given cluster are formed solely as a result of collisional processes (Leigh et al., 2007).

In order to predict the frequency of BSSs in the core of GCs as a function of age, we have created a semi-analytic, highly approximate model to perform the necessary calculations. By comparing the predictions of our simple model to the trends observed in the (Piotto et al., 2002) database, we hope to constrain the relevant rates that govern BSS production in GC cores, specifically those pertaining to collisions, coalescence, and mass segregation.

We can approximate the number of BSSs in the core at a given time-step, t_{dyn}, using the formula:

$$N_{BSS} = N_{collisions} + N_{mergers} + N_{in} - N_{out} - N_{destroyed}, \tag{5.1}$$

where $N_{collisions}$ is the number of collisionally-produced BSSs with each time-step, $N_{mergers}$ is the number of BSSs formed via binary coalescence, N_{in} is the number of BSSs that migrate into the core with each time-step, N_{out} is the number of BSSs that migrate out of the core, and $N_{destroyed}$ is the number of BSSs that reach the end of their lifetimes with each time-step. We have assumed a dynamical time-step of $t_{dyn} = 1.0 \times 10^9$ years so that most clusters are assumed to have undergone on the order of ten such dynamical times over the course of their lives.

The number of BSSs expected to migrate out of the core with each time-step can be expressed as:

$$N_{out} = \frac{N_{BSS_0}}{N_{core}} r_{out} t_{dyn} \tag{5.2}$$

The rate of stellar evaporation from the core is denoted by r_{out}, whereas N_{core} and N_{BSS_0} represent, respectively, the total number of stars in the core and the total number of BSSs in the core. For simplicity, however, we have assumed $r_{out} = 0$ as a first approximation since, due to the slightly higher masses of BSSs relative to the majority of the other single stars in the core, we expect few, if any, BSSs to migrate out of the core once inside.

The number of BSSs expected to migrate into the core with each time-step can be written:

$$N_{in} = r_{in} t_{dyn} \tag{5.3}$$

The rate of stellar migration into the core is denoted by r_{in}. We note that most of the BSSs formed outside of the core must primarily be the result of binary mergers, and much less of collisions. Both single-binary and binary-binary encounters can be neglected outside of the core as only a small fraction of these interactions will occur there (Davies, 1995).

There appears to be no relation between the relative frequency of central BSSs and that of their external counterparts (in the outskirts) (e.g. Mapelli et al., 2006). As such, our estimate for the rate of inward migration is taken from the equipartition timescale:

$$t_{eq} = \frac{m_{star}}{m_1 + m_2 - 0.1} t_h, \tag{5.4}$$

where m_{star} is the average stellar mass and is taken to be 0.5 $M_\odot$. The term $m_1 + m_2 - 0.1$ is meant to represent the average BSS mass resulting from the merger of two stars having masses m_1 and m_2. Note that we expect around 0.1 $M_\odot$ to be lost from the system in a typical merger event and that we have adopted $m_1 = 0.5$ $M_\odot$ and $m_2 = 0.8$ $M_\odot$. The rate of inward migration into the core is given by:

$$r_{in} = 1.0/t_{eq} \tag{5.5}$$

The total number of stellar collisions per time-step can be written:

$$N_{collisions} = N_{1+1} + N_{1+2} + N_{2+2}, \tag{5.6}$$

where N_{1+1} is the number of collisions between 2 single stars, N_{1+2} is the number of collisions between a single star and a binary pair, and N_{2+2} is the number of collisions between 2 binaries.

The number of single star collisions per time-step, N_{1+1}, can be approximated as:

$$N_{1+1} = r_{1+1} t_{dyn}, \tag{5.7}$$

The rate of single star collisions (number of collisions per cluster per year) is given by (Piotto et al., 2004):

$$r_{1+1} = \frac{1}{\tau_{1+1}}, \tag{5.8}$$

and τ_{1+1} is given by Equation 4.21.

The ratio of the number of BSSs produced via single-single collisions to the number produced via single-binary collisions appears to be a sensitive function

of both the cluster concentration and the initial mass function (IMF) (Davies, 1995). The rate of collisions between single stars and binary systems can nonetheless be roughly approximated as:

$$r_{1+2} = \frac{1}{\tau_{1+2}}, \tag{5.9}$$

where τ_{1+2} is the timescale required for single-binary encounters to occur as given by Equation 4.22. As in Equation 5.7, the number of single-binary collisions per time-step, N_{1+2}, can be approximated as:

$$N_{1+2} = r_{1+2} t_{dyn} \tag{5.10}$$

A similar logic can be implemented to approximate the rate of collisions between binary pairs (2+2 encounters). As with 1+2 interactions, in order to be dynamically significant, encounters between two binaries require a minimum separation that is comparable to the orbital separation of the binaries themselves ($R_{min} \simeq d$) (Davies, 1996). The expression for the rate of binary-binary encounters should bear a striking resemblance to that for single-binary encounters:

$$r_{2+2} = \frac{1}{\tau_{2+2}} \tag{5.11}$$

τ_{2+2} is given by Equation 4.23 and is nearly three orders of magnitude smaller than τ_{1+1}. We have included an additional factor of 10 in τ_{2+2} so that Equation 4.23 applies to a binary fraction of 10%, which we feel is a good starting point and is representative of many GCs, though clearly precise binary fractions remain largely unknown and are expected to fluctuate. By incorporating such a high f_b, we expect to over-count the number of binary-binary encounters occurring in the core. The rate of binary mergers is a function of not only

the binary fraction, but also of the distribution of orbital periods and separations as well as of the masses of the individual stellar components. Both MS and post-MS binary interactions can result in coalescence and if the final mass of the merger product exceeds the cluster turn-off mass, a blue straggler is created.

Mergers can occur within a Hubble time to form a single MS star only in tight binaries having short periods ($\lesssim 5$ days) and low mass components (one of which must be smaller than 1.2 $M_{\odot}$) (Andronov et al., 2006). In the case of wide binaries having long periods ($\gtrsim 5$ days), the timescale for orbital decay is too large and mass transfer can be initiated once the primary has left the MS. Binaries having sufficiently long periods (wide separations) have larger collisional cross-sections and so tend to undergo more encounters. Soft binaries, for which the total binding energy of the system satisfies $|E|/m_a\sigma^2 < 1$, have wide separations (with periods of months or even years) and are thought to get wider, or softer, as they evolve due to dynamical processes and should not be able to produce BSSs via mass transfer (Binney & Tremaine, 1987). On the other hand, hard binaries, for which $|E|/m_a\sigma^2 > 1$, are thought to shift to lower periods post-encounter and ultimately merge earlier on in the cluster's lifetime (Heggie, 1975). Assuming a central velocity dispersion of around 10 km/s, one can estimate that any binary in the core having a separation greater than ≈ 2.2 AU will inevitably experience a disruptive encounter with a neighboring star long before it will have had time to merge. We therefore assume that only binaries having semi-major axes less than 2.2 AU will merge.

The total number of binary mergers occurring in the core can be approximated at each time-step as:

$$N_{mergers} = f_{merge} r_{merge} t_{dyn} \tag{5.12}$$

The fraction of binaries that will actually merge is represented by f_{merge}. If we assume a flat distribution in the number of binaries versus log P, and that typical binary separations range from 0.01 AU (in contact) to 30 AU (anything larger is rapidly destroyed via dynamical processes), then no matter the bin size we chose, the same number of binaries will fall into each (Sills & Bailyn, 1999). Consequently, the fraction of binaries that will merge can be approximated by:

$$f_{merge} = 2.2AU/(30AU - 0.01AU), \tag{5.13}$$

or $f_{merge} = 0.0734$. r_{merge} is the rate of binary mergers (number per year) found by taking the inverse of the timescale for a single merger event and then multiplying by the number of potential mergers, or:

$$r_{merge} = \frac{N_b}{t_{merge}} \tag{5.14}$$

The total number of binaries in the core, N_b, is given by:

$$N_b = \frac{f_b N_{core}}{2}, \tag{5.15}$$

where N_{core} is the total number of stars in the core, and the binary fraction, f_b, is assumed to be 10%. We have chosen a slightly lower-than-normal f_b in order to properly account for the fact that a significant fraction of those binaries will comprise stars having a mass-ratio that could not possibly result

in blue straggler formation, or at least not ones that will live long enough to have any chance of being observed. We let t_{merge} represent the time in years required for a single merger event to take place in a binary system having an initial separation of $a = 2.2$ AU, or:

$$t_{merge} = \frac{a}{\dot{a}} \tag{5.16}$$

The rate of decay for the orbital separation is taken from Equation 4.27, though we ignore the effects of spin angular momenta on the total loss of angular momentum from the system as a first approximation. If we assume a typical mass-loss rate of around 10^{-10} $M_{\odot}$ per year for a low-mass MS star with a binary companion, we find that it is the mass-transfer process itself that seems to primarily drive the orbital decay. This mass-loss rate does not seem unreasonable given that a solar-like star without a binary companion is expected to lose mass at a rate of around 10^{-14} $M_{\odot}$ per year. In order to get an idea of realistic estimates for the rate of angular momentum loss from a typical binary system that could ultimately result in the production of a BSS, various mass ratios and average stellar properties were considered. However, on average, we expect stars with ≈ 0.5 $M_{\odot}$ and ≈ 0.5 $R_{\odot}$ to occur with the highest frequency in a typical GC. We have also chosen 0.5 $M_{\odot}$ for the mass of the accretor and 0.8 $M_{\odot}$ for the mass of the donor star, which generate comparable rates of angular momentum loss to what is obtained for other mass ratios that could similarly result in the formation of a blue straggler star.

Finally, the number of BSSs destroyed with each time-step is a function of the number of BSSs left over after the previous time-step, as well as of

the fraction expected to reach the end of their lives within t_{dyn}. This can be written:

$$N_{destroyed} = \frac{t_{dyn}}{t_{BSS}} N_{BSS_0}, \tag{5.17}$$

where N_{BSS_0} is the number of BSSs calculated to populate the core at the end of the last time-step, and t_{BSS} represents the average BSS lifetime and is assumed to be 1.5×10^9 years (Lombardi et al., 2002). If we were to choose t_{dyn} such that $t_{dyn}/t_{BSS} \geq 1.0$, we could assume that all of the BSSs leftover at the end of the last time-step are destroyed by the end of the next one.

In this model, rates are assumed to be constant over the course of a cluster's lifetime. While this may not be entirely accurate, it is not too far from the truth in post-core collapse clusters and certainly provides a good starting point for our model. Dynamical effects should alter both the binary fraction and binary orbital parameters as the system evolves, which could potentially affect the rate of BSS production in the core. As a first approximation, we assume that the rate of binary destruction is comparable to the rate of creation and so maintain a fixed binary fraction throughout the evolution of the cluster. While this may not be representative of what goes on in real GCs, we have to start somewhere. In order to implement a more realistic treatment of binary evolution, however, a better understanding of the various dynamical processes that operate in GCs and how they interact is needed.

5.2 Preliminary Results and Discussion

The simple model previously described was designed to predict the number of BSSs in the core as a function of cluster age. The older the cluster, the

more dynamical time-steps it will have undergone. We set out to find some link between BSS formation and environment and so paid particularly close attention to which cluster parameters factored into our estimates of BSS formation rates. Our goal was to be able to more or less reproduce the observed trends between BSS frequency and the various cluster parameters considered, namely total mass, central density, central velocity dispersion, half-mass relaxation time, etc. Given the simplicity of the assumptions made, we were hoping to find a reasonably good agreement between observed BSS numbers and those predicted by our model, though were forced to concede that such an outcome was idealistic and would more than likely not be the case.

Interestingly, our model predicted BSS frequencies that were in surprisingly good agreement with the observations. In fact, roughly two-thirds of the BSS populations predicted by our model agree or nearly agree with the observations, within error. Figure 5.1 shows the relation between the number of BSSs predicted by our model for each cluster and the number observed. Calculations were only carried out for clusters for which we had both reliable relative age estimates and central velocity dispersions and so only 24 data points are shown. Note that in most clusters, our model more or less reproduces what we see.

We compared our predictions to global cluster properties like the cluster luminosity (total mass), central density, central velocity dispersion, half-mass relaxation time, etc. We hoped to be able to reproduce the observed trends, first and foremost, but also wanted to better understand what we were seeing. For instance, the more half-mass relaxation times a cluster has undergone, the

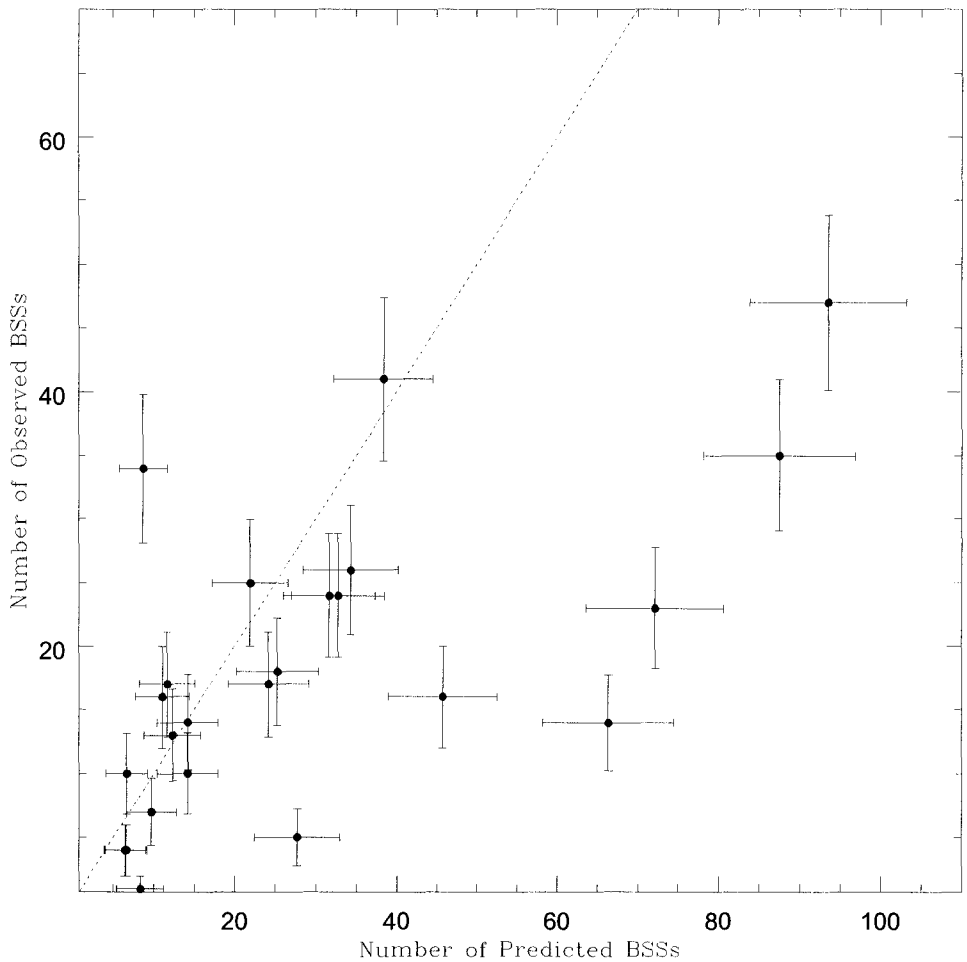

Figure 5.1: Plot of the number of core BSSs observed in Piotto et al.'s 2002 database versus the number predicted by our model. The dashed line represents the 1:1 line or perfect agreement between theory and observations. Error bars were done using Poisson statistics.

more dynamically evolved it should be. We were not entirely certain how this might affect BSS production and were specifically concerned with whether or not their numbers rise steadily as a function of dynamical times, or whether some equilibrium is reached where BSS formation rates become balanced with the rate of their destruction/outward migration. In the end, we were surprised to find trends that matched up rather well with the observed ones, as shown in Figure 5.2, Figure 5.4, and Figure 5.3.

We also compared the number of BSSs predicted by our crude model to both collisional parameters considered in Chapter 3, namely Γ_1 and Γ_2 which are given by Equation 3.26 and Equation 3.27, respectively. We observe more or less the same general trends as we did upon comparing the theoretical collision rates to observed BSS frequencies. One could argue for the existence of weak anti-correlations, particularly with Γ_2. As was the case with the observations, however, such a correlation is speculative at best. Figure 5.5 shows the relation between both collisional parameters and the results of our model.

We reiterate how surprised we were to find such a reasonably good agreement between the predictions of our highly simplified model and the observations. The only real discrepancy occurred in the plots for central density. We saw no evidence for an anti-correlation between F_{BSS} and ρ_0 in the observations; however, our model suggests otherwise and at first glance seems indicative of increased densities somehow impeding BSS formation. While it remains difficult to pin-point the exact cause of the disagreement, we found this particular trend odd in light of the fact that our model predicts that most

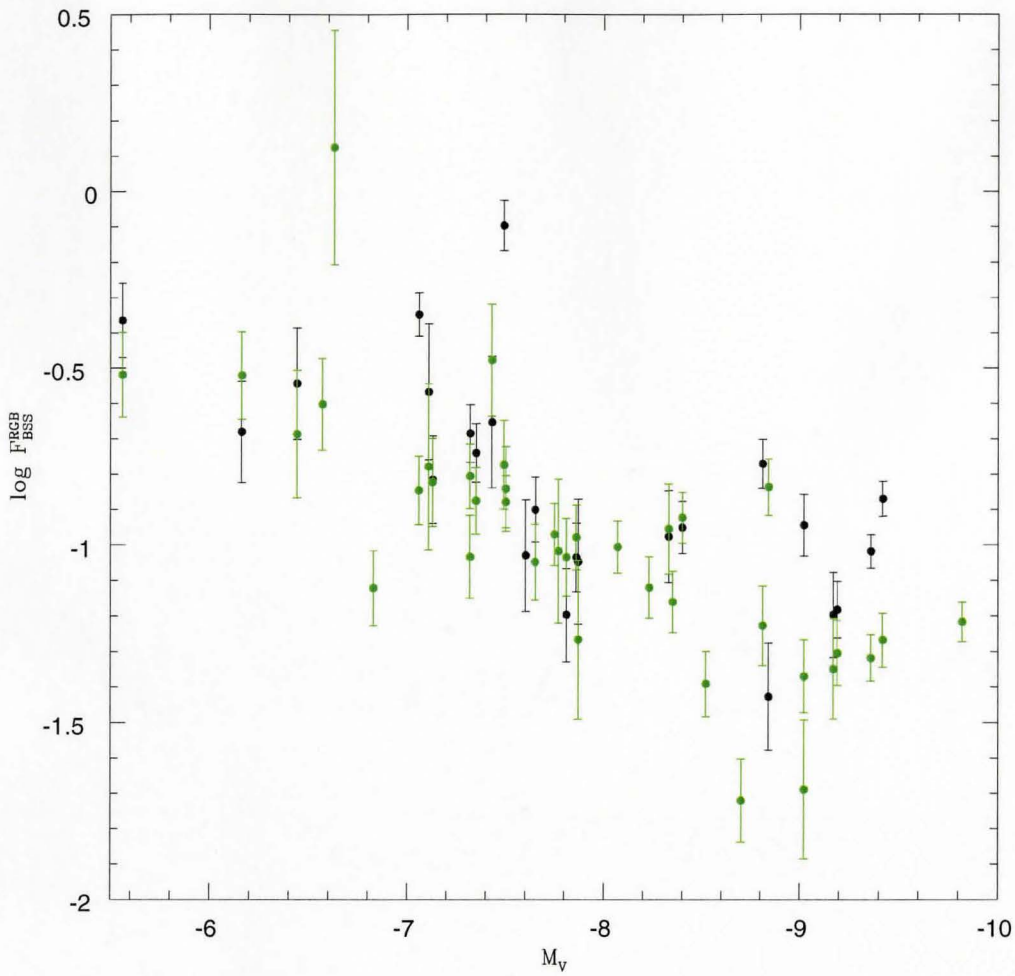

Figure 5.2: Plot of our model predictions for the core BSS frequency versus the total cluster V magnitude (black dots). Frequencies were normalized using RGB star counts taken from the Piotto et al. (2002) database. For easy comparison, we have included the observed frequencies (green dots). Note the anti-correlation that exists between F_{BSS} and the total cluster mass in both the observations and our model predictions. Error bars were calculated using Poisson statistics.

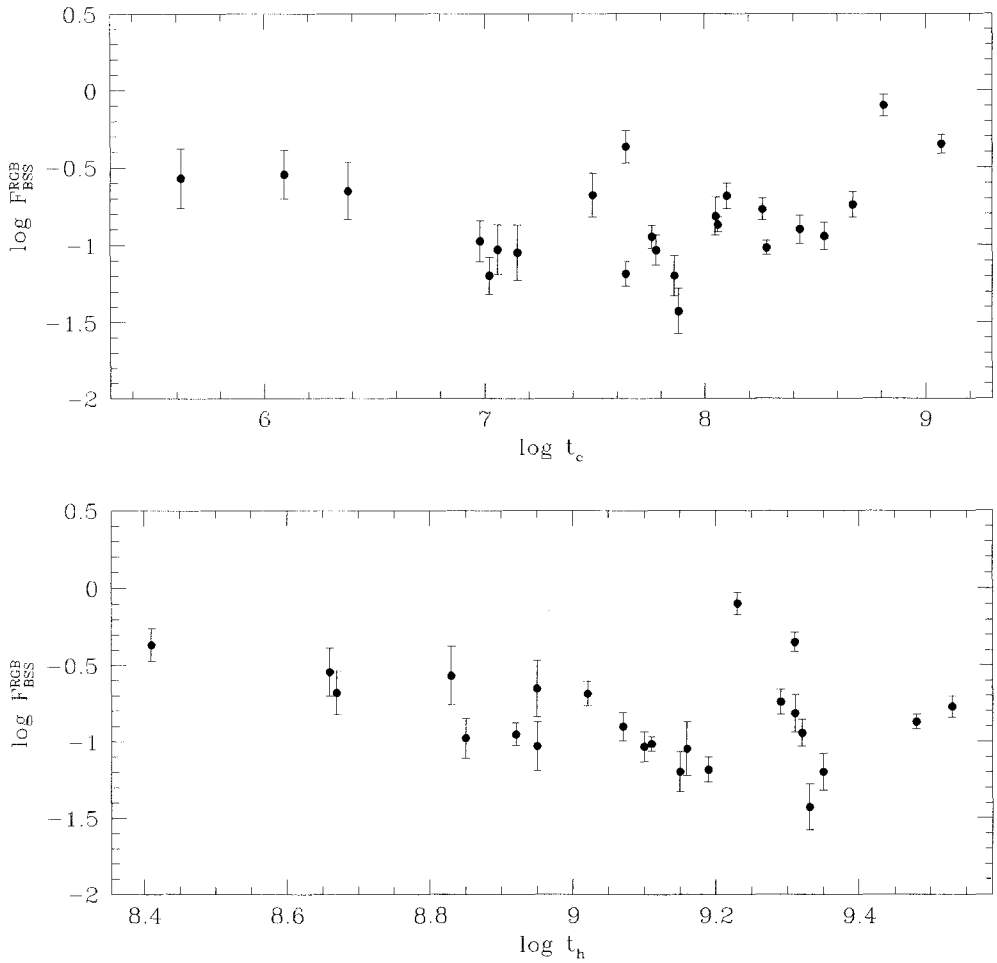

Figure 5.3: Plot of our model predictions for the core BSS frequency versus the logarithm of the core relaxation time in years (top), and the logarithm of the relaxation time at the half-mass radius in years (bottom). Frequencies were normalized using RGB star counts taken from the Piotto et al. (2002) database. Note the weak anti-correlation that exists between F_{BSS} and log t_h. Error bars were calculated using Poisson statistics.

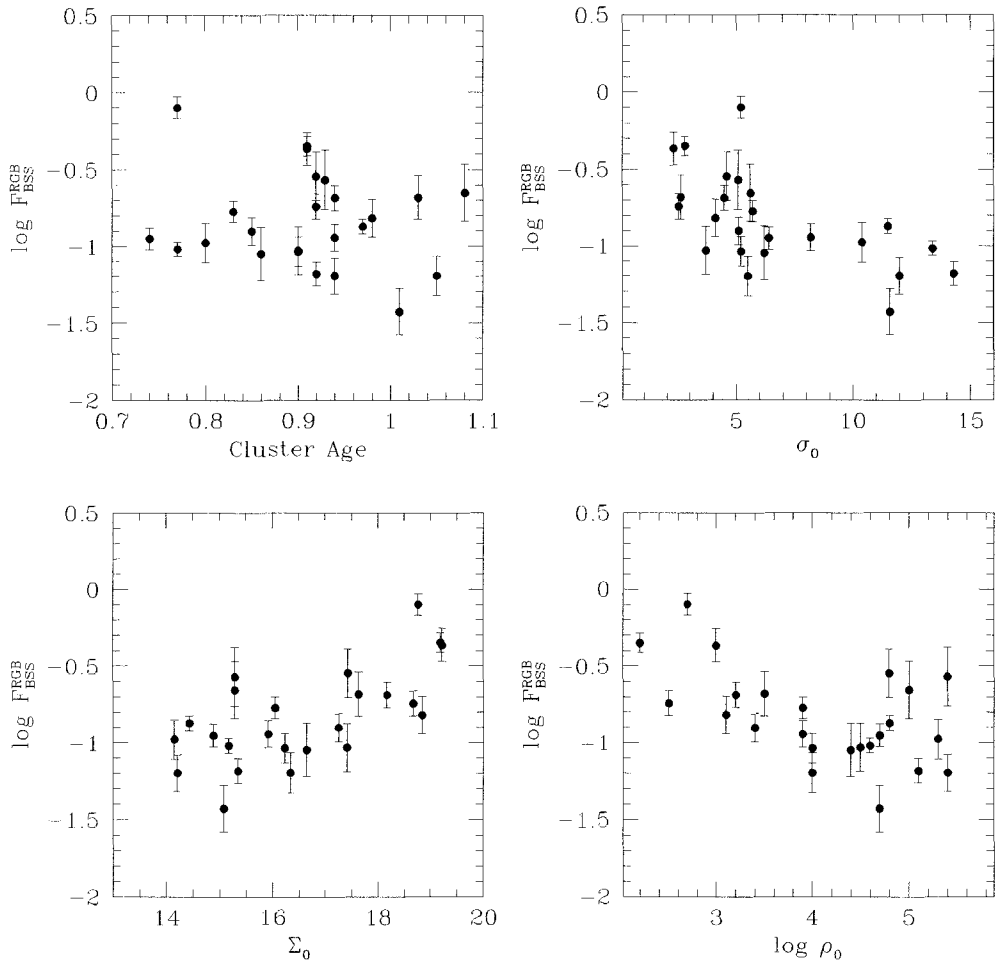

Figure 5.4: Plots of our model predictions for the core BSS frequency versus the logarithm of the central density (bottom right), the central surface brightness (bottom left), the relative cluster age (top left), and the central velocity dispersion (top right). Frequencies were normalized using RGB star counts taken from the Piotto et al. (2002) database. The central density is given in units of $L_\odot$ pc^{-3}, the central surface brightness in units of V mag arc $second^{-2}$, and the central velocity dispersion in units of km s^{-1}. The cluster age is normalized, however, and its values represent the ratio between the cluster age and the mean age of a group of metal-poor clusters, namely 11.2 Gyrs, as described in De Angeli et al. (2005). Error bars were calculated using Poisson statistics.

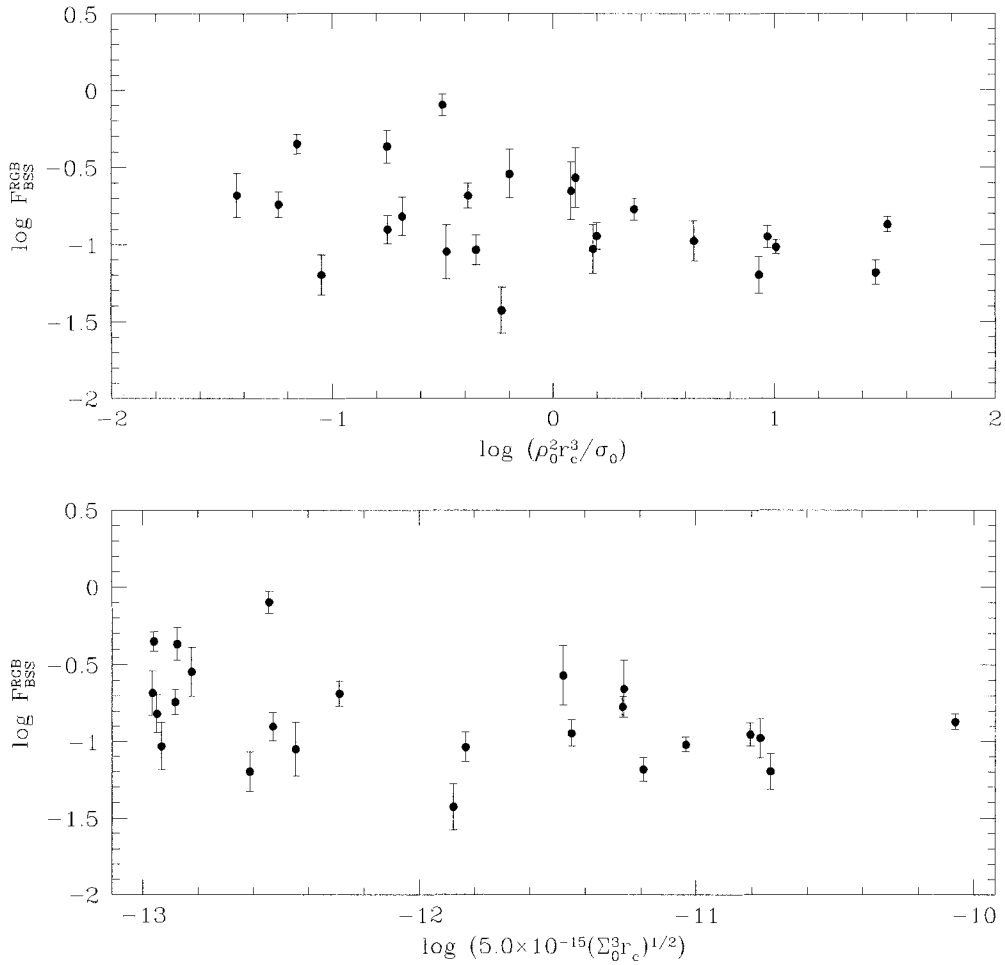

Figure 5.5: Plot of our model predictions for the core BSS frequency versus the logarithm of collisional parameter Γ_1 (bottom), and the logarithm of collisional parameter Γ_2 (top). Frequencies were normalized using RGB star counts taken from the Piotto et al. (2002) database. Error bars were calculated using Poisson statistics.

core BSSs are a direct result of binary coalescence in tight binaries having small separations, a mechanism that was chosen to operate independently of the cluster density. With only a small contribution to the total number of core BSSs stemming from collisions, we suspect that the predicted anti-correlation with ρ_0 is an artifact of our model and is purely coincidental.

Sills & Bailyn (1999) incorporated a crude representation of cluster dynamics and detailed binary-single star encounter simulations using smoothed particle hydrodynamics in order to generate collisional-cross sections and rates. The evolution of the collision products were then tracked using the Yale stellar evolution code in order to predict BSS distributions in colour-magnitude diagrams. After applying the results of their model to available data from the core of M3, they were unable to reproduce the observed BSS population under a single, albeit consistent, set of assumptions. Collisions do not appear to be solely responsible for BSS formation, even in clusters in which they are thought to be occurring the most. The results of Sills & Bailyn (1999) are thus not in complete contradiction to our own, though we predict a much smaller collisional contribution to the overall BSS population. Nonetheless, we find it interesting that models in which collisions are assumed to be the primary culprits behind BSS formation tend to have difficulty in reproducing the observations. While models that rely entirely on mass-transfer for BSS production do not necessarily paint a complete picture, there are still a great number of uncertainties pertaining to merger rates that need to be addressed, most notably concerning the binary fraction. The observational and theoretical data currently available seem to point towards the importance of obtaining

more reliable estimates for the rate of binary coalescence in gaining a better understanding of BSS formation.

Mapelli et al. (2006) created a model similar to, albeit more complicated than, our own in order to predict the final locations of BSSs in the cluster in order to generate simulated radial distributions for comparison with the observed ones. Their code follows the dynamical evolution of the BSS population in the gravitational potential of four different GCs modeled using a multi-mass King density profile, taking into consideration both the influence of dynamical friction and the effects of distant encounters. They looked at about 10 different cases for each cluster, making the total number of runs on the order of 400,000. Ultimately, they found that both mass-transfer in PBs and MS mergers due to collisions (in the core) must coexist and operate with comparable efficiency in low and high density clusters. In M3, 47 Tuc, and NGC 6752 in particular they found that the mass-transfer BSSs are slightly less numerous than their collisional counterparts, but can be found all throughout the cluster. In the case of Omega Centauri, however, they believe that the majority of the BSSs come from PBs. Mapelli et al. speculate that in this particular case, the lack of collisionally-produced BSSs could be a consequence of mass segregation having not yet migrated enough PBs towards the cluster center. The results of our own model do not entirely disagree with those of Mapelli et al. (2006), though we predict fewer collisionally-produced BSSs overall. It is entirely possible that our model under-predicts the number of collisions occurring in the clusters above the 1:1 line in Figure 5.1, which would in turn generate a better agreement between our predictions and the observations. If this is indeed the

case, the results of our own simplified model could be made to more or less agree with those of the more complicated simulations of Mapelli et al. (2006).

Additionally, it seems that by simply adjusting the binary fraction, a better agreement between our model predictions and the observations can be attained. We have found that by increasing f_b, we can in turn increase the number of hard binaries in our model and hence observe a corresponding increase in F_{BSS}. In other words, by lowering f_b from 10% to around 2-5%, we can shift those points under the 1:1 line in Figure 5.1 to obtain a better agreement with the data. Similarly, by similarly increasing f_b, we can shift over those points above the 1:1 line. More work still needs to be done, though the preliminary results of our model point towards a possible dependence of F_{BSS} on the binary fraction. Indeed, a good test of the validity of our model could come from superior and more abundant measurements of the binary fractions in GCs.

In future work, we would also like to look at varying the rates of migration into and out of the core in order to gain a better understanding of how this might affect F_{BSS} therein. Accurately predicting inward migration rates depends on which dynamical processes are operating with the greatest frequencies in the cluster outskirts, which should in turn affect the BSS production rates in these outer regions. A general agreement is found in the literature that in these outer regions, most BSSs are the result of PB mergers, though it remains difficult to gauge how formation rates in the central cluster regions will differ from those in the outskirts due to a lack of reliable estimates in the literature (e.g. Mapelli et al., 2006). Consequently, a great deal of uncertainty

still surrounds the internal migration rates of BSSs and how such processes could potentially relate to the observed bimodal distribution of these enigmatic stars (e.g. Ferraro et al., 1997).

Bibliography

Andronov, N., Pinsonneault, M. H., & Terndrup, D. M. 2006, ApJ, 646, 1160

Bailyn, C. D. & Pinsonneault, M. H. 1995, ApJ, 439, 705

Binney, J. & Tremaine, S. 1987, Galactic dynamics (Princeton, NJ, Princeton University Press)

Davies, M. B. 1995, MNRAS, 276, 887

Davies, M. B. 1996, in IAU Symp. 174: Dynamical Evolution of Star Clusters: Confrontation of Theory and Observations, ed. P. Hut & J. Makino, 243

De Angeli, F., Piotto, G., Cassisi, S., Busso, G., Recio-Blanco, A., Salaris, M., Aparicio, A., & Rosenberg, A. 2005, AJ, 130, 116

Djorgovski, S. 1993, in ASP Conf. Ser. 50: Structure and Dynamics of Globular Clusters, ed. S. G. Djorgovski & G. Meylan, 373

Ferraro, F. R., Beccari, G., Rood, R. T., Bellazzini, M., Sills, A., & Sabbi, E. 2004, ApJ, 603, 127

Ferraro, F. R., Paltrinieri, B., Fusi Pecci, F., Cacciari, C., Dorman, B., Rood, R. T., Buonanno, R., Corsi, C. E., Burgarella, D., & Laget, M. 1997, A&A, 324, 915

Heggie, D. C. 1975, MNRAS, 173, 729

Leigh, N., Sills, A., & Knigge, C. 2007, ArXiv Astrophysics e-prints, astro-ph/0702349

Lombardi, Jr., J. C., Warren, J. S., Rasio, F. A., Sills, A., & Warren, A. R. 2002, ApJ, 568, 939

Mapelli, M., Sigurdsson, S., Colpi, M., Ferraro, F. R., Possenti, A., Rood, R. T., Sills, A., & Beccari, G. 2004, ApJ, 605, L29

Mapelli, M., Sigurdsson, S., Ferraro, F. R., Colpi, M., Possenti, A., & Lanzoni, B. 2006, MNRAS, 373, 361

Piotto, G., De Angeli, F., King, I. R., Djorgovski, S. G., Bono, G., Cassisi, S., Meylan, G., Recio-Blanco, A., Rich, R. M., & Davies, M. B. 2004, ApJ, 604, L109

Piotto, G., King, I. R., Djorgovski, S. G., Sosin, C., Zoccali, M., Saviane, I., De Angeli, F., Riello, M., Recio-Blanco, A., Rich, R. M., Meylan, G., & Renzini, A. 2002, A&A, 391, 945

Sigurdsson, S., Davies, M. B., & Bolte, M. 1994, ApJ, 431, L115

Sills, A. & Bailyn, C. D. 1999, ApJ, 513, 428

Chapter 6

Summary

In this thesis, we wanted to investigate the relationship between blue straggler formation and cluster environment. Specifically, we wished to explore the effects of various dynamical processes on blue straggler frequencies within the cores of globular clusters. By focussing on the densest cluster regions we hoped to isolate primarily collisionally-produced BSS populations, though were surprised to find that the observations failed to support our hypothesis.

We used the homogeneous database of HST globular cluster photometry from Piotto et al. (2002) to look for relationships between relative BSS frequencies and global cluster properties. We found an anti-correlation between the total integrated cluster luminosity (total mass) and F_{BSS} in the core, as well as between the central velocity dispersion and F_{BSS}. A weak anti-correlation was found with the half-mass relaxation time, though it appears to flatten beyond $\log t_h = 9.0$. No other robust trends were found between relative BSS frequencies and any other cluster parameter, including any collisional parameters.

Cumulative BSS luminosity functions were analyzed for all 57 GCs. Unlike Piotto et al. (2004), we found no real difference between the BSLFs of the most massive clusters and those of the least massive clusters and found no correlation between the shape of the cumulative LFs and any other cluster property. These results seem to suggest that either the products of both formation mechanisms have indistinguishable luminosity functions, or a single formation mechanism is operating predominantly in all environments.

With the above results in mind, we designed a very simple model in an attempt to reproduce the observed trends. As such, we set out to predict the number of BSSs found in the cores of GCs as a function of the various formation mechanisms. Our initial expectation was that by considering only those stars in the dense cores of GCs, we would isolate a more or less entirely collisionally-produced BSS population. According to the data, however, relatively few BSSs are thought to be the products of direct collisions. No correlations were found with any global cluster parameters that might be indicative of an environment characteristic of frequent collisions, in particular no trends were found with the central density or any collisional parameters. In fact, the observed trends are consistent with collisional processes somehow impeding BSS production in GC cores, though we cannot conclude that such a process is responsible for the observed correlations, or lack thereof. The observations, as well as the results of our crude model, seem to indicate that tight binaries with short periods are responsible for the majority of the BSSs that we see.

More of our model's parameter space should be explored. We were surprised to find such a good agreement between theory and observations due to

the simplicity of our model. Indeed, it reproduced all but one of the observed trends. The only discrepancy occurred with the central density - our model predicted an anti-correlation with F_{BSS} though such a trend was not observed. At this point, however, we can say that the relatively good agreement between our model predictions and the data could be indicative of the importance of binary mergers in BSS formation. It is possible that the surprisingly similar observational and theoretical trends, or lack thereof, seen between F_{BSS} and various global cluster properties suggests that relative BSS frequencies are more or less independent of their environment and are more a function of the total number (or mass) of stars and the binary fraction.

More observations are needed in order to better constrain the frequencies with which the various dynamical processes are occurring in GCs. Specifically, we need more numerous and more reliable measurements of binary fractions. Clearly, if most of the BSSs that we observe in GCs are the products of coalescence in binary systems, then we would expect to see a correlation between F_{BSS} and f_b.